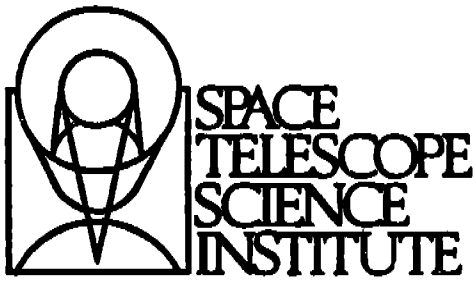

Hubble Space Telescope

Faint Object Spectrograph

Instrument Handbook

There is a corrigenda inserted inside the front cover of this document. It effects pages 19, 26 and 58.

Version 2.0
April 1992

Revision History

Handbook Version 1.0	October 1985; edited by Holland Ford
Handbook Version 2.0	May 1989; edited by Anne L. Kinney

The Space Telescope Science Institute is operated by the Association of Universities for Research in Astronomy, Inc., for the National Aeronautics and Space Administration.

FAINT OBJECT SPECTROGRAPH

INSTRUMENT HANDBOOK

Version 2.0
April, 1992

A.L. Kinney

Space Telescope Science Institute
3700 San Martin Drive
Baltimore, MD 21218

CONTENTS

INTRODUCTION 1

1.0 INSTRUMENT CAPABILITIES 2

1.1 Spectral Resolution 3
1.2 Exposure Time Calculations 6
1.3 Brightness Limits 19
1.4 Time Resolution 19
1.4.1 ACCUM 20
1.4.2 RAPID 20
1.4.3 PERIOD 21
1.5 Polarization 22
1.6 FOS Noise and Dynamic Range 22

2.0 OBSERVING MODES 25

2.1 Acquiring the Target: ACQ 25
2.1.1 INT ACQ 26
2.1.2 ACQ/BINARY 27
2.1.3 ACQ/PEAK 27
2.1.4 ACQ/FIRMWARE 28
2.1.5 WF/PC Assisted Target Acquisition 28
2.1.6 Examples 29
2.1.7 Acquisition Exposure Times 31
2.2 Taking Spectra: ACCUM and RAPID 33

3.0 INSTRUMENT PERFORMANCE AND CALIBRATIONS 34

3.1 Wavelength Calibrations 34
3.2 Absolute Photometry 34
3.3 Flat Fields 34
3.4 Sky Lines 35

4.0 SIMULATING FOS 41

5.0 ACKNOWLEDGEMENTS 43

6.0 REFERENCES 44

APPENDIX A. TAKING DATA WITH FOS 45

APPENDIX B. DEAD DIODE TABLES 48

APPENDIX C. A COMPARISON OF GHRS AND FOS SENSITIVITIES 52

APPENDIX D. GRATING SCATTER 54

APPENDIX E. EXPOSURE LOGSHEETS 56

LIST OF TABLES

Table 1.0.1 FOS at a Glance 5
Table 1.1.1 FOS Dispersers 7
Table 1.1.2 FOS Apertures 8
Table 1.1.3 FOS Line Widths (FWHM) as a Function of Aperture Size 10
Table 1.2.1 FOS Observed Counts Sec^{-1} $Diode^{-1}$ for Point Sources at Wavelength λ .. 15
Table 1.2.2 Counts sec^{-1} $diode^{-1}$ for representative spectral types at 15th magnitude . 16
Table 1.3.1 Brightness Limits 19
Table 2.1.1 FOS Visual Magnitude Limits with Camera Mirror 29
Table 2.1.2 Total Exposure Times for FOS Firmware 32
Table 2.1.3 Minimum Exposure Times 33
Table 4.1 Example parameters in SYNPHOT to reproduce Figure 1.2.3 42
Table A.1 FOS Observing Parameters 46
Table B.1 FOS Dead and Noisy Channel Summary 49
Table B.2 FOS Dead and Noisy Channels History 50
Table C.1 GHRS and FOS Sensitivities 53

LIST OF FIGURES

Figure 1.0.1 Quantum efficiency of the FOS Flight detectors 3
Figure 1.0.2 A schematic optical diagram of the FOS 4
Figure 1.1.1 A schematic of the FOS apertures projected onto the sky 9
Figure 1.1.2 Spectral line spread functions for various FOS apertures 11
Figure 1.2.1 HST+FOS Efficiency, E_λ vs. λ 12
Figure 1.2.2 Light transmitted by apertures for a centered point source 14
Figure 1.2.3 Detected counts-s^{-1}-$diode^{-1}$ for input spectrum 17
Figure 1.5.1 FOS waveplate retardation and polarimeter transmission 23
Figure 1.6.1 Measured count rate versus true count rate 24
Figure 2.1.0 Slews performed after FOS target acquisition 25
Figure 3.3.1 Redside G160L Data of target G191-B2B 36
Figure 3.3.2 Redside G190H Data of target G191-B2B 37
Figure 3.3.3 Redside G270H Data of target G191-B2B 38
Figure 3.3.4 Blueside G190H Flat Field of target G191-B2B 39
Figure 3.3.5 Redside G190H Flat Field of target G191-B2B 40
Figure D.1 Comparison of FOS and GHRS 16 Cyg B HST spectra 55

INTRODUCTION

Section 1 attempts to present all information that is needed for proposing to observe with the FOS, *i.e.* for filling out Phase I Proposals. The overall instrument capabilities are described and presented in Table 1.0.1. The spectral resolution is given in Section 1.1 as a function of grating and aperture. The data for calculating exposure times is given in Section 1.2 in three different ways. The easiest way to calculate exposure time is by simply reading off the detected counts s^{-1} $diode^{-1}$ in a given grating when illuminated by a constant input spectrum of $F = 1.0 \times 10^{-14}$ erg cm^{-2} s^{-1} $Å^{-1}$ (Figure 1.2.3). The count rate can then be normalized to the expected incident flux of the object of interest. The limits for the brightest objects that can be observed with FOS is given in Section 1.3. A discussion of time resolution with the FOS, *i.e.* ACCUM, RAPID, and PERIOD modes, is given in Section 1.4. Polarization is discussed in Section 1.5. The FOS noise and dynamic range are discussed in Section 1.6.

Section 2 attempts to present much of the information that is needed for observing with the FOS after winning HST time, *i.e.* for filling out Phase II Proposals. The acquisition of targets is described in Section 2.1. Examples of the exposure logsheets that have been validated by the Remote Proposal System (RPS) are given for target acquisition (for example, ACQ/BINARY mode). Exposure logsheets examples are also given for ACCUM mode, for RAPID mode, and for spectropolarimetry (observed in ACCUM mode with the optional parameter STEP-PATT = POLSCAN). Exposure logsheets can be found in Appendix E.

Section 3 briefly describes the current wavelength calibration, absolute photometry, and flat field calibrations of FOS. The data used to produce the flat fields are shown.

Section 4 describes how to simulate FOS spectra with the "synphot" package which runs in the ST Data Analysis System (STSDAS) under IRAF. A version of the simulator compatible with VAX/VMS machines (XCAL) is also available to be copied from an anonymous ftp account at ST ScI. The simulators, developed by K. Horne, are useful tools since they allow input of a large variety of spectra and they incorporate the current calibration files for the FOS.

The actual details of taking data are given in Appendix A, along with the FOS observing parameters both in the nomenclature of exposure logsheets, and in the nomenclature of FOS headers. Most importantly, Appendix A gives the equations for calculating the start time of any time resolved exposure. Appendix B lists the dead diode tables of April 13, 1992. Appendix C is a comparison of GHRS and FOS sensitivities by Gilliland & Hartig (1991). Appendix D summarized the results of tests of scattered red light into the blue side detectors by Caldwell & Cunningham (1992). Observing red objects in the ultraviolet with FOS can be problematical because of scattered red light.

1.0 INSTRUMENT CAPABILITIES

The Faint Object Spectrograph and its use is fully described in the Version 1.0 FOS Instrument Handbook (Ford 1985) and in the supplement to the Instrument Handbook (Hartig 1989), from which much of this handbook is drawn. The detectors are described in detail in Harms *et al.* 1979, and Harms 1982.

The general traits of FOS blue side (FOS/BL) and red side (FOS/RD) are given in Table 1.0.1, along with those of the GHRS for comparison. For further reference, Appendix C contains the ST ScI Newsletter article by Gilliland & Hartig (1991) *A Comparison of GHRS and FOS Sensitivities.*

The Faint Object Spectrograph has two Digicon detectors with independent optical paths. The Digicons operate by accelerating photoelectrons emitted by the transmissive photocathode onto a linear array of 512 diodes. The individual diodes are 0.36″ wide along the dispersion direction and 1.43″ tall perpendicular to the dispersion direction. The detectors span the wavelength range on the blue side from 1150Å to 5400Å (FOS/BL) and on the red side from 1620Å to 8500Å (FOS/RD). The quantum efficiency of the two detectors is shown in Figure 1.0.1. The optical diagram for the FOS is given in Figure 1.0.2. The FOS entrance apertures are placed 3.6′ from the optical axis of HST.

Gratings are available with both high spectral resolution (1 to 6Å diode^{-1}, $\lambda/\Delta\lambda \approx$ 1300) and low spectral resolution (6 to 25Å diode^{-1}, $\lambda/\Delta\lambda \approx 250$). The actual spectral resolution depends on the point spread function of HST, the dispersion of the grating, the aperture used, and whether the target is physically extended.

The instrument has the ability to take spectra with high time resolution ($\geq$ 0.03 seconds, RAPID mode) and the ability to bin spectra in a periodic fashion (PERIOD mode). The FOS also has polarimetric capabilities on the blue side, and, with the upcoming correction to geomagnetically induced image drift, should have its polarimetric capabilities restored on the red side. However, no polarimetry is anticipated after the installation of the Corrective Optics (COSTAR) because of the strong instrumental polarization introduced.

There is a large aperture for acquiring targets using on-board software (4.3″ × 4.3″). A variety of science apertures are available; a large aperture for collecting the maximum light (effectively 4.3″ × 1.4″); a slit for optimizing spectral resolution (effectively 0.25″ × 1.4″); and several circular apertures (1.0″, 0.5″, and 0.3″) and paired square apertures (1.0″, 0.5″, 0.25″, and 0.1″) for isolating spatially resolved features and for subtracting sky.

The point spread function of HST has lowered the effective spectral resolution of FOS and caused throughput losses, so that the smallest apertures are not presently useful. There are also several additional problems with the instrument. The magnetic shielding on the red detector is insufficient, so that the geomagnetic field causes the image on the photocathode to drift as much as a diode width as a function of position in orbit and of telescope pointing. A similar image drift exists on the blue side, but to a smaller degree, a factor of $\approx$ 4 times smaller than the red side. The image drift is predictable, and because spectra are read out often in ACCUM mode (every two minutes on the red side, every 4 minutes on the blue side) image drift for both sides can be removed in STSDAS software after the observations. The drift is scheduled to be corrected for both sides in orbit by adjusting the magnetic field of the detectors according to the position in orbit, and direction of pointing, in the fall of 1992. The blue side sensitivity appears to be decreasing at a rate of about 10% per year. The red side sensitivity is stable overall but has been observed to decrease in a highly

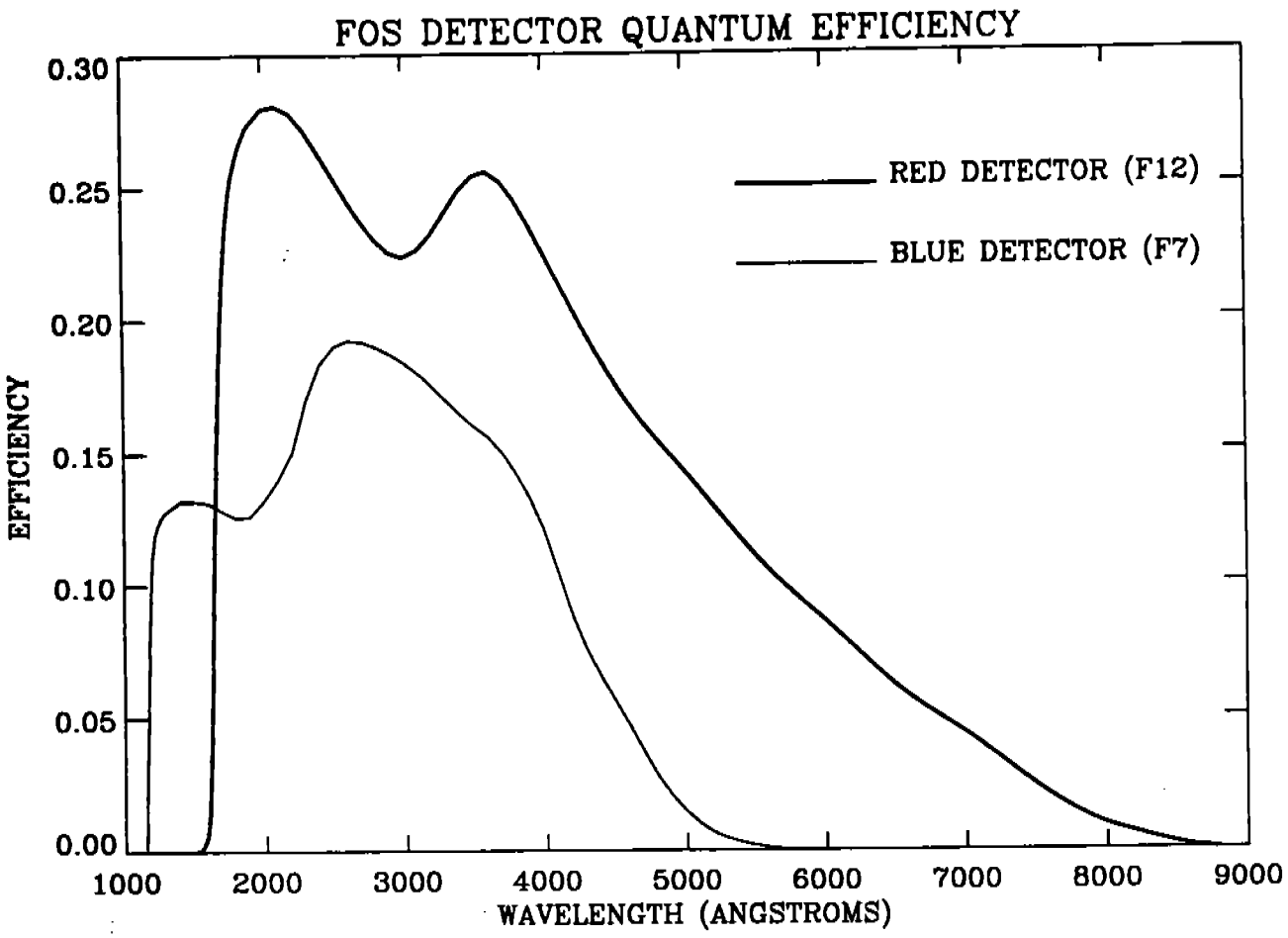

Figure 1.0.1: Quantum efficiency of the FOS Flight detectors.

wavelength dependent fashion between 1800Å and 2100Å affecting gratings G190H, G160L, and to a lesser degree G270H. Flat fields have been obtained in the large aperture (effectively $4.3'' \times 1.4''$) every month since January 1992, and will be taken bi-monthly in both the large aperture and in the slit, so that a library of flat fields is being built up to assist in the removal this effect (see Figures in Section 3). The sensitivity of both the blue and the red detectors is being monitored $\approx$ every 3 months.

1.1 Spectral Resolution

The spectral resolution depends on the point spread function of the telescope, the dispersion of the grating, the aperture, and whether the target is extended or is a point source. Table 1.1.1 lists the gratings, their wavelengths, and their dispersions (Kriss, Blair, & Davidsen 1991). All available FOS apertures are listed in Table 1.1.2 with their designation as given in HST headers, their size, and shape. Figure 1.1.1 shows the FOS entrance apertures overlaid upon each other together with the diode array. The positions of the apertures are accurately known and highly repeatable.

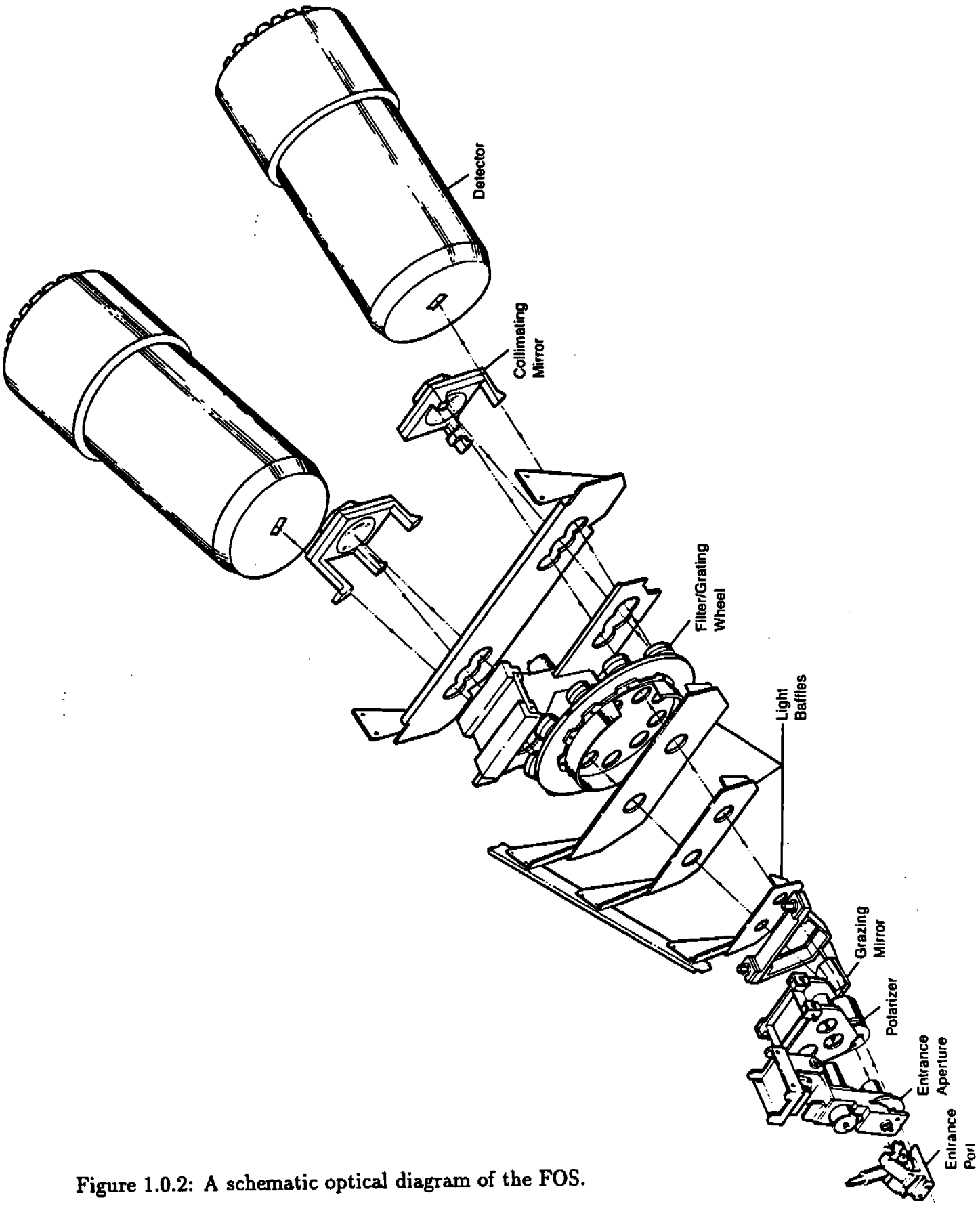

Figure 1.0.2: A schematic optical diagram of the FOS.

Table 1.0.1
FOS at a Glance

Wavelength coverage[1]	FOS/BL: 1150Å to 5400Å in several grating settings.
Wavelength coverage	FOS/RD: 1620Å to 8500Å in several grating settings.
Spectral resolution	High: $\lambda/\Delta\lambda \approx 1300$.
Spectral resolution	Low: $\lambda/\Delta\lambda \approx 250$.
Highest time resolution	$\Delta t \geq 0.03$ seconds.
Acquisition aperture	$4.3'' \times 4.3''$
Science apertures[2]	Largest – Effectively $4.3'' \times 1.4''$,
	Smallest – $0.1''$ square paired,
	Most used – Effectively $0.25'' \times 1.4''$ slit
Brightest observable stars[3]	$V \approx 8$ for B0V, $V \approx 4$ for G2V.
Dark count rate	FOS/BL: 0.007 counts s^{-1} $diode^{-1}$.
	FOS/RD: 0.01 counts s^{-1} $diode^{-1}$.
Example exposure time[4]	$F_{1300} = 2.5 \times 10^{-13}$, SNR=20/(1.0Å), t=2500s
	$F_{2800} = 1.3 \times 10^{-13}$, SNR=20/(2.0Å), t=70s (FOS/BL)
	$F_{2800} = 1.3 \times 10^{-13}$, SNR=20/(2.0Å), t=50s (FOS/RD)

GHRS at a Glance

Wavelength coverage, resolution[5]	1100Å to 3200Å $\lambda/\Delta\lambda = 20,000$.
	With $\approx$ 40Å coverage per grating setting.
Wavelength coverage, resolution	1680Å to 3200Å $\lambda/\Delta\lambda = 100,000$.
	With $\approx$ 10Å coverage per grating setting.
Highest time resolution	$\Delta t \geq 0.05$ seconds.
Large science aperture (LSA)	$2.0'' \times 2.0''$.
Small science aperture (SSA)	$0.25'' \times 0.25''$.
Brightest acquireable stars	$V \approx 4$ for B0V, $V \approx -5$ for G2V.
Dark count rate	0.01 counts s^{-1} $diode^{-1}$.
Example exposure time[6]	$F_{1300} = 2.5 \times 10^{-13}$, SNR=20/(0.065Å), t=2000s
	$F_{2800} = 1.3 \times 10^{-13}$, SNR=20/(0.14Å), t=1000s

[1] See Table 1.1.1 for grating dispersions and wavelength coverage.
[2] See Table 1.1.2 for available apertures.
[3] See Table 1.3.1 for brightest observable objects, which are strongly dependent on spectral type and grating.
[4] See Section 1.2 for exposure time calculations, and Table 1.2.1 for count rates for objects with a variety of spectral types. The example given here is for 3C273.
[5] See the GHRS Instrument Handbook for details.
[6] The example given here is for 3C273, from Morris *et al.* 1991.

The spectral resolution (FWHM) is given as a function of aperture in Table 1.1.3 in units of diodes for a point source at 3000Å and for a uniform, extended source. The FWHM does not vary strongly as a function of wavelength, so that this FWHM, together with the dispersion of the gratings given in Table 1.1.2, can be used to approximate the effective spectral resolution. For example, a point source observed on the red side with the G270H grating in the (effective) $4.3'' \times 1.4''$ aperture has a spectral resolution of

$$\text{FWHM} = 1.50 \text{ diode} \times 2.05\text{Å diode}^{-1}$$

$$\text{FWHM} = 3.08\text{Å}.$$

The same observation in the $0.25'' \times 2.0''$ slit would have a spectral resolution of

$$\text{FWHM} = 1.08 \text{ diode} \times 2.05\text{Å diode}^{-1}$$

$$\text{FWHM} = 2.21\text{Å}.$$

The line spread functions computed from a model point spread function at 2250Å in the FOS apertures are shown in Figure 1.1.2 in units of microns, where 1 diode = 50 microns.

1.2 Exposure Time Calculations

The information necessary to calculate exposure time is given here in several forms. First, the HST + FOS efficiencies (Figure 1.2.1), aperture throughputs (Figure 1.2.2), and wavelength dispersions (Table 1.1.1) are given together with a series of relations between count rate and input spectra (Table 1.2.1). Then, count rate per diode at the wavelength corresponding approximately to the peak sensitivity of the given grating is given in tabular form for a few spectral types for 15^{th} magnitude objects (Table 1.2.2). Finally, the count rate per diode is shown in Figure 1.2.3 for both detectors and all gratings, assuming a flat input spectrum ($F_\lambda \propto \lambda^0 = 1.4 \times 10^{-14}$ erg cm^{-2} s^{-1} Å^{-1}) observed in the (effective) $4.3'' \times 1.4''$ aperture.

For example, the count rate for an object with flux of $F_\lambda = 3.5 \times 10^{-15}$ erg cm^{-2} s^{-1} Å^{-1} at 3700Å using the red detector, in the (effective) $4.3'' \times 1.4''$ aperture with the G400H grating, is given by equation 1 in Table 1.2.1.

$$N_\lambda = 2.28 \times 10^{12} F_\lambda (\lambda \Delta\lambda) E_\lambda T_\lambda$$

where $F_\lambda = 3.5 \times 10^{-15}$ erg cm^{-2} s^{-1}, $\lambda = 3700$Å, $\Delta\lambda = 3.0$Å (from Table 1.1.1), the efficiency is $E_\lambda = 0.0065$ (from Figure 1.2.1), and the throughput is $T_\lambda = 0.68$ (from Figure 1.2.2), so that

$$N_\lambda = 3.9 \text{ counts s}^{-1}\text{diode}^{-1}.$$

The exposure time for a desired signal-to-noise ratio per resolution element is then given by $t = SNR^2$ counts diode$^{-1}/N_\lambda$ counts sec^{-1} diode^{-1}, which for $SNR = 20$, is $t = 400/3.9$ counts sec^{-1} diode^{-1} = 103 s.

As a comparison, count rates for objects of representative spectral type with $V = 15.0$ are given in Table 1.2.2 at the wavelengths corresponding to the peak response of a given

Table 1.1.1
FOS Dispersers

Grating	Diode No. at Low λ	Low λ (Å)	Diode No. at High λ	High λ (Å)	Δλ (Å-Diode^{-1})	Blocking Filter
			Blue Digicon			
G130H	60	1150[1]	516[7]	1606	1.00	--
G190H	1	1573	516	2330[4]	1.47	--
G270H	1	2222	516	3301	2.09	SiO_2
G400H	1	3240	516	4823	3.07	WG 305
G570H	1	4575	516	6872[3]	4.45	WG 375
G160L	318	1150[1]	516	2510[4]	6.87	--
G650L	295	3540	373	9022[3]	70.28	WG 375
PRISM	175	1850[2]	24	5500[3]	--	--
			Red Digicon*			
G190H	516	1565[5]	1	2312[5]	-1.45	--
G270H	516	2223	1	3278	-2.05	SiO_2
G400H	516	3238	1	4784	-3.00	WG 305
G570H	516	4571	1	6820	-4.37	WG 375
G780H	516	6272	1	9219[6]	-5.72	OG 530
G160L	126	1600[5]	1	2430	-6.64	--
G650L	205	3540	1	8729	-25.44	WG 375
PRISM	332	1850	497	8950[6]	--	--

[1] The blue Digicon's MgF_2 faceplate absorbs light shortward of 1150 Å.
[2] The sapphire prism absorbs light shortward of 1650 Å; however, because of the large dispersion of the prism at the shortest wavelengths, the effective cutoff is longward of 1650 Å.
[3] Quantum efficiency of the blue tube is very low longward of 5500 Å.
[4] The second order overlaps the first order longward of 2300 Å, but its contribution is at a few percent.
[5] The red Digicon's fused silica faceplate strongly absorbs light shortward of 1650 Å.
[6] Quantum efficiency of the red detector is very low longward of 8600 Å.
[7] The photocathode electron image typically is deflected across 5 diodes, effectively adding 4 diodes to the length of the diode array

* Wavelength direction is reversed for the red side relative to the blue side.

Table 1.1.2
FOS Apertures

Designation (Header Designation)	Number	Shape	Size (″)	Separation (″)	Special Purpose
0.3 (B-2)	Single	Round	0.30 dia	NA	Spectroscopy and Spectropolarimetry
0.5 (B-1)	Single	Round	0.50 dia	NA	Spectroscopy and Spectropolarimetry
1.0 (B-3)	Single	Round	1.00 dia	NA	Spectroscopy and Spectropolarimetry
0.1-PAIR (A-4)	Pair	Square	0.10	3.0	Object and Sky
0.25-PAIR (A-3)	Pair	Square	0.25	3.0	Object and Sky
0.5-PAIR (A-2)	Pair	Square	0.50	3.0	Object and Sky
1.0-PAIR (C-1)	Pair	Square	1.00	3.0	Extended Objects
0.25 x 2.0 (C-2)	Single	Rectangular	0.25 x 2.0	NA	High Spectral Resolution
0.7 x 2.0-BAR (C-4)	Single	Rectangular	0.7 x 2.0	NA	Surrounding Nebulosity
2.0-BAR (C-3)	Single	Square	2.0	NA	Surrounding Nebulosity
BLANK (B-4)	NA	NA	NA	NA	Dark and Particle Events
4.3 (A-1)	Single	Square	4.3	NA	Target Acquisition and Spectroscopy
Failsafe	Pair	Square	0.5 and 4.3	NA	Target Acquisition and Spectroscopy

The first dimension of rectangular apertures is along the dispersion direction, and the second dimension is perpendicular to the dispersion direction. The two apertures with the suffix designation "BAR" are bisected by an occulting bar which is 0.3" wide in the direction perpendicular to the dispersion.

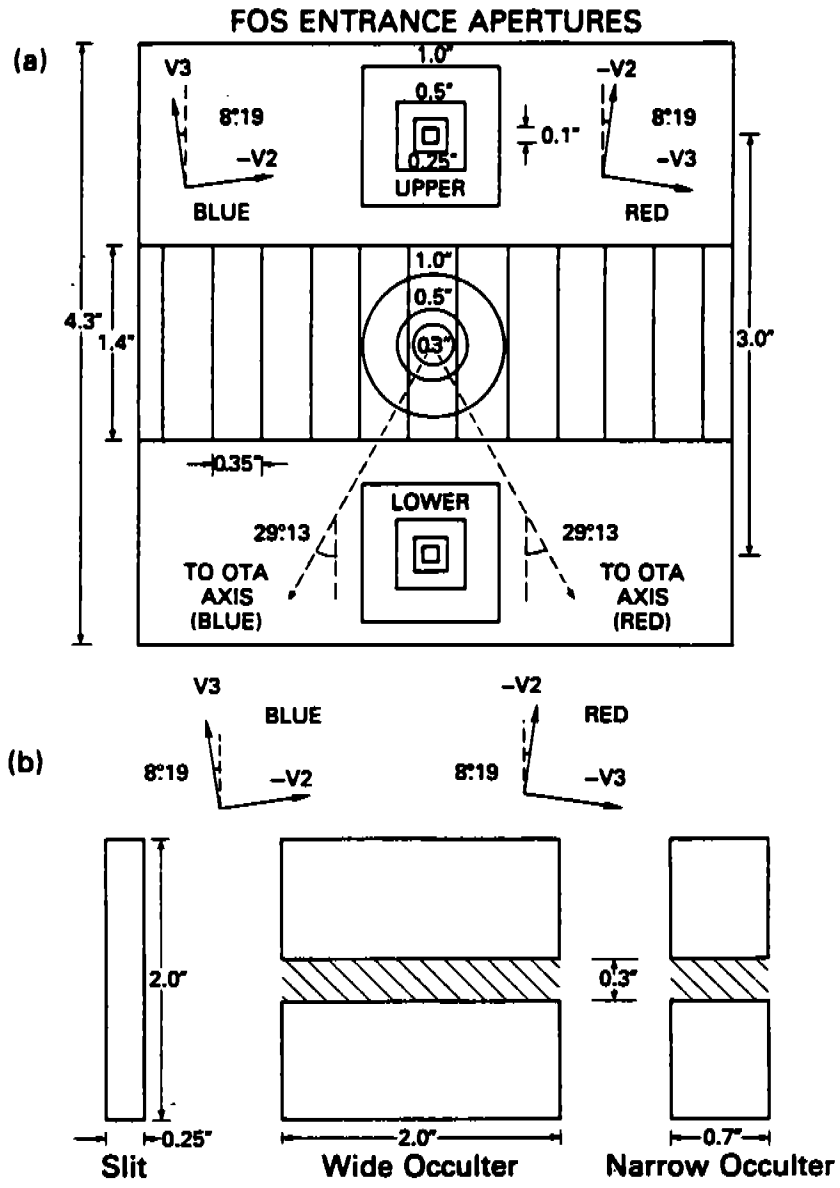

Figure 1.1.1: A Schematic of the FOS Apertures projected onto the sky. The upper panel shows the array of $0.35'' \times 1.4''$ diodes projected across the center of the $4.3'' \times 4.3''$ target acquisition aperture. The target acquisition aperture and the single circular apertures position to a common center. The pairs of square apertures position to common centers with respect to the target acquisition aperture as shown in the figure. Either the upper aperture (the "A" aperture, which is furthest from the HST optical axis) or the lower aperture (the "B" aperture, which is closest to the HST optical axis) in a pair can be selected by an appropriate y-deflection in the Digicon detectors. The lower panel shows the three acquisition slits; two of the slits are bisected by an $0.3''$ opaque occulting bar. The centers of the three slits position to the center of the target acquisition aperture. The figure shows the orientation of the direction perpendicular to the dispersion in the HST V2, V3 focal plane on the blue and red sides. The FOS x-axis is parallel to the diode array and positive to the left; the y-axis is perpendicular to the diode array and positive toward the upper aperture.

Table 1.1.3
FOS Line Widths (FWHM) as a Function of Aperture Size

Designation	Size (")	Uniform Source		Point Source at 3000A
		G130H (Blue)	G570H (Red)	
0.3	0.3 (circular)	1.00 ± .01	0.95 ± .02	1.06
0.5	0.5 (circular)	1.27 ± .04	1.20 ± .01	1.14
1.0	1.0 (circular)	2.29 ± .02	2.23 ± .01	1.34
0.1-PAIR	0.10 (square)	0.97 ± .03	0.92 ± .02	1.00
0.25-PAIR	0.25 (square)	0.98 ± .01	0.96 ± .01	1.00
0.5-PAIR	0.50 (square)	1.30 ± .04	1.34 ± .02	1.18
1.0-PAIR	1.00 (square)	2.65 ± .02	2.71 ± .02	1.40
0.25 X 2.0	0.25 X 2.0 (slit)	0.99 ± .01	0.96 ± .01	1.00
0.7 X 2.0-BAR	0.70 X 2.0	1.83 ± .02	1.90 ± .01	1.30
2.0-BAR	2.0	5.28 ± .07	5.43 ± .04	1.40
4.3	4.3(square)	-	-	1.50

The FWHM are given in units of diodes.

grating. The example given above corresponds to an object with power law $F_\nu \propto \nu^{-2}$, V=15.0, observed with the G400H grating on the red side.

The count rate for observations in the (effective) $4.3'' \times 1.4''$ aperture can be read directly from Figure 1.2.3 and scaled to the appropriate flux. For the example given above, with $F_\lambda = 3.5 \times 10^{-15}$erg cm^{-2}s^{-1}Å^{-1}, the count rate per diode at 3700 Å is given by $N_\lambda = (3.5 \times 10^{-15}/1.0 \times 10^{-14}) \times 10. = 3.5$ counts s^{-1} diode^{-1}. To calculate the count rate in other science apertures, the count rate must be multiplied by the throughputs in Figure 1.2.2.

When observing in time resolved modes, the total observing time can become dominated by the read–out time for FOS data. Section 1.4 below discusses the time to read–out the FOS in the context of RAPID observations.

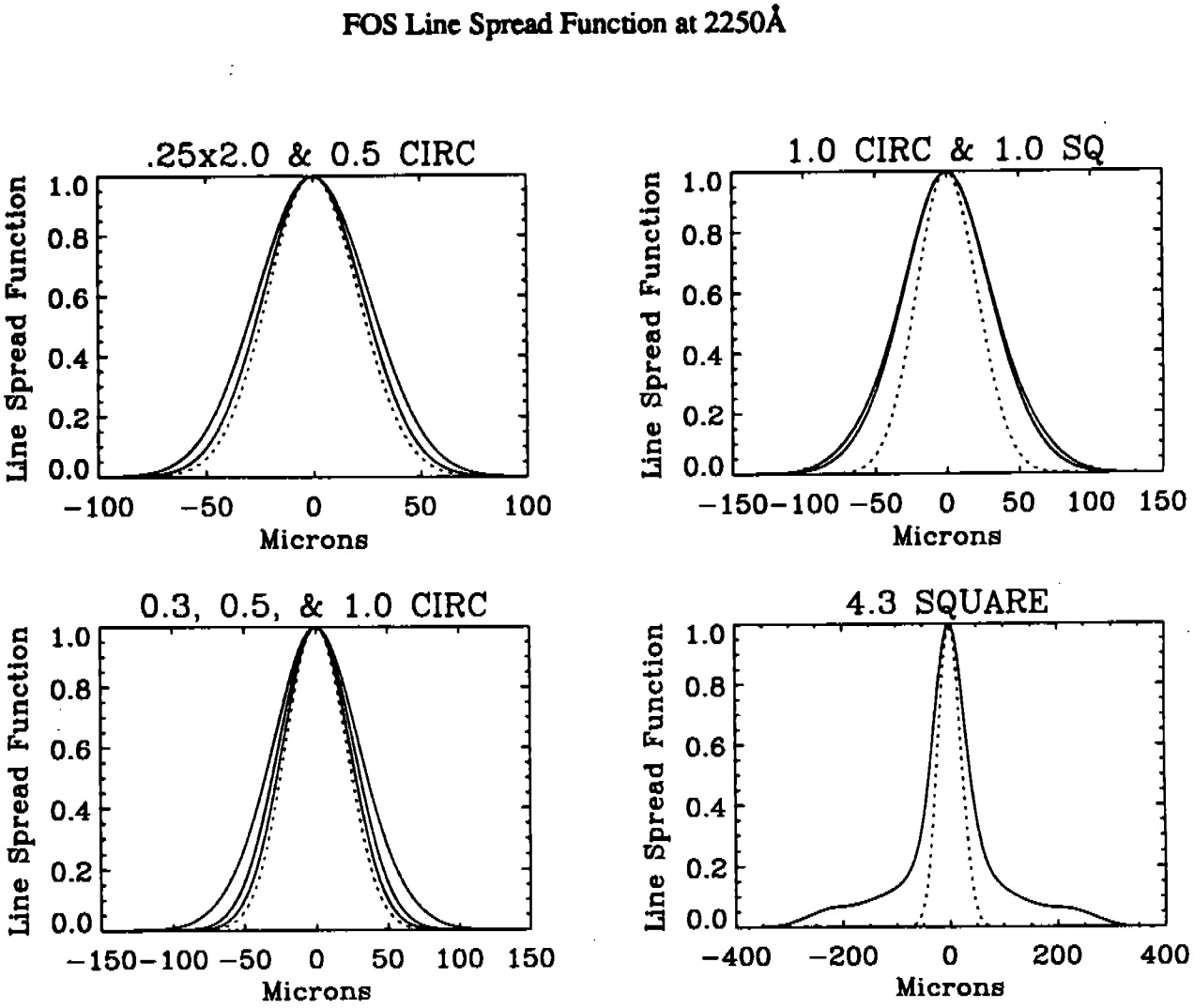

Figure 1.1.2: The solid curves are spectral line spread functions for various FOS apertures. Ordinate shows relative intensity versus distance in the dispersion direction in microns (one diode, equal to one nominal spectral resolution element, is 50 microns). FOS instrument profile is shown by the dotted line. Smearing of the profiles is due to spherical aberration.

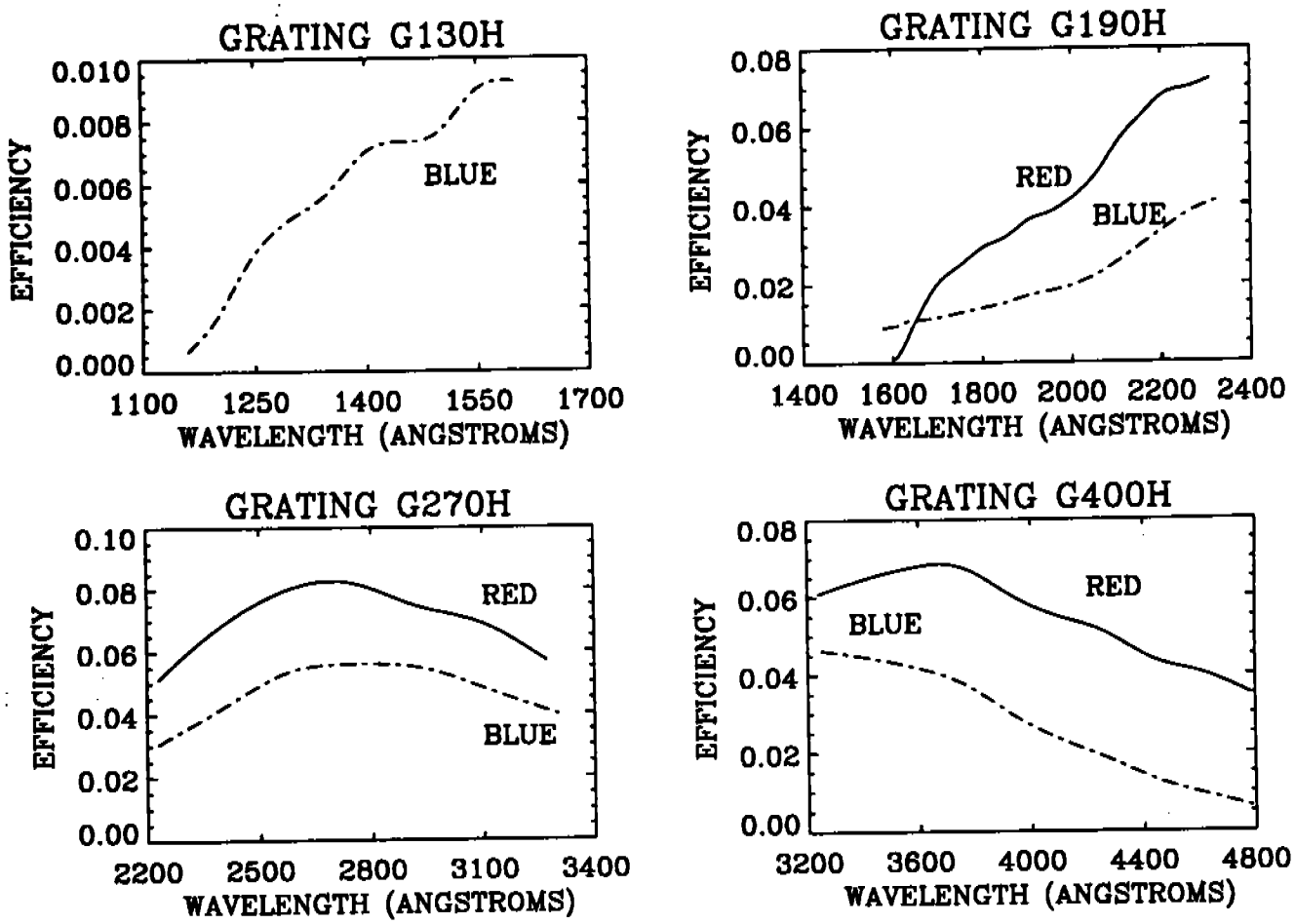

Figure 1.2.1: HST+FOS Efficiency, E_λ vs. λ.

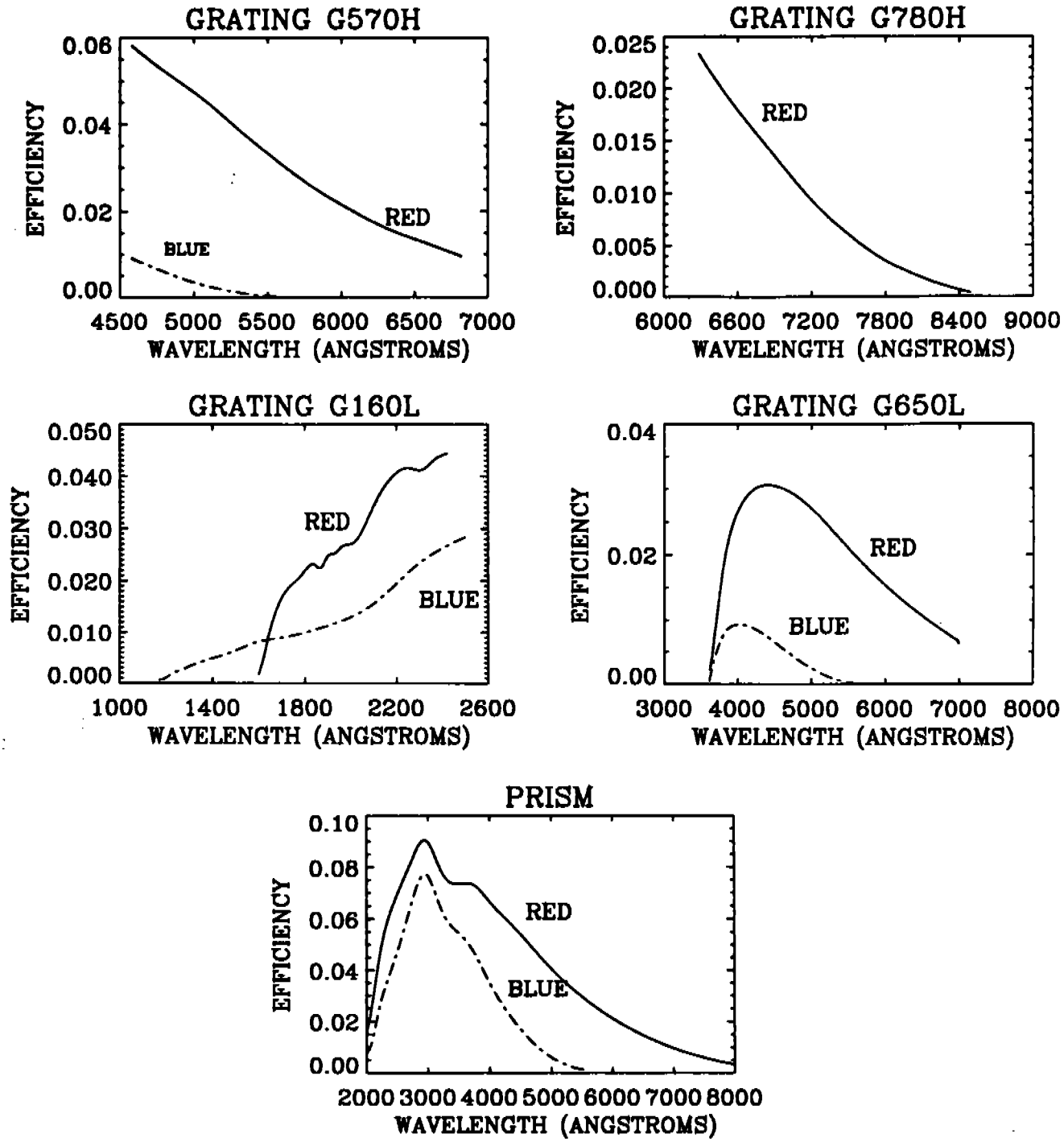

Figure 1.2.1 (*Continued*): HST+FOS Efficiency, E_λ vs. λ.

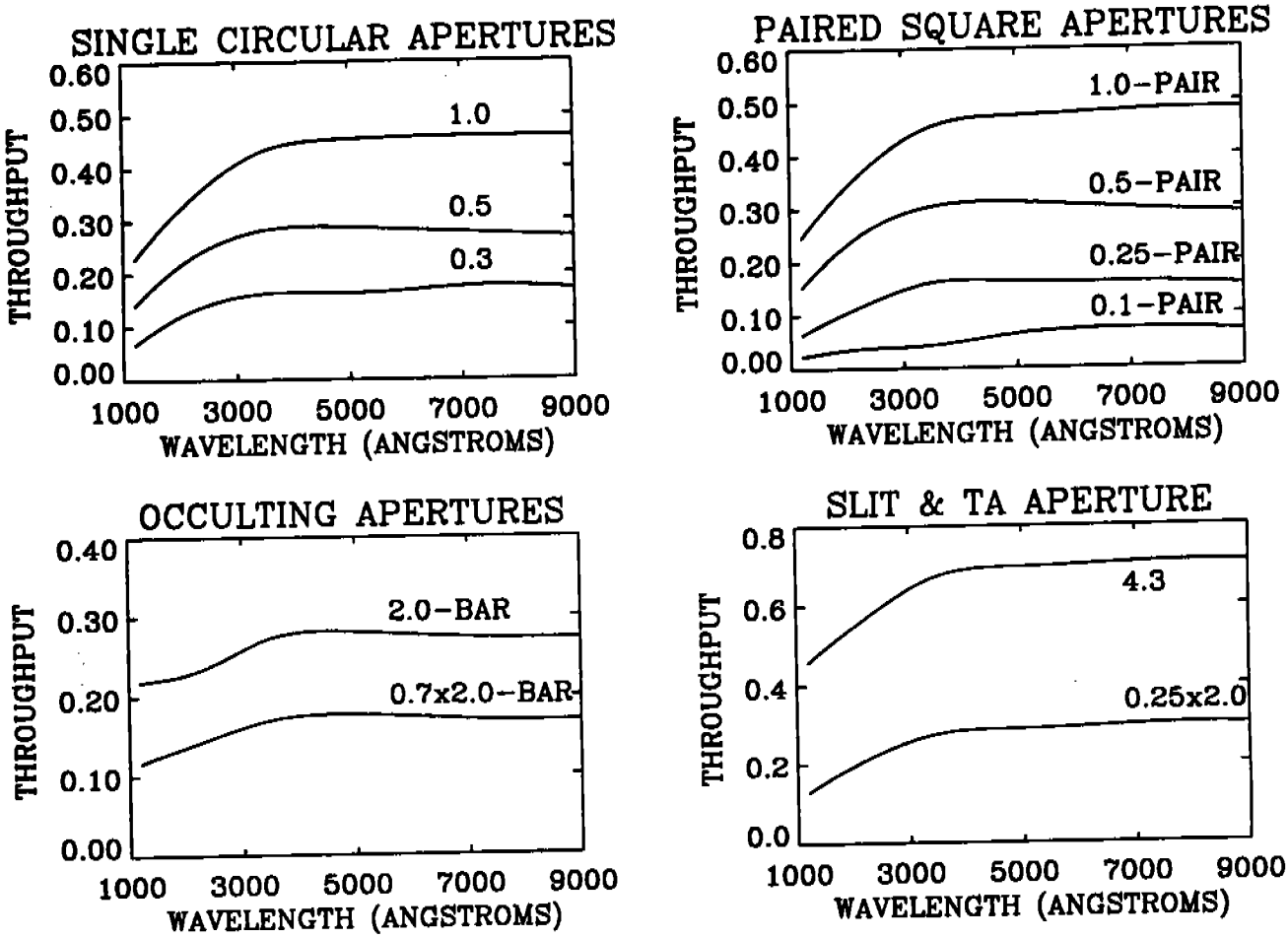

Figure 1.2.2: Fraction of light transmitted by the apertures for a perfectly centered point source.

Table 1.2.1

FOS Observed Counts Sec^{-1} $Diode^{-1}$ (N_λ) for Point Sources at Wavelength λ (Å)

Flux Distribution	Inputs	Equation for N_λ (counts- sec^{-1} $diode^{-1}$)
1. Continuum	F_λ(ergs cm^{-2} s^{-1} $Å^{-1}$)	$2.28 \times 10^{12} F_\lambda \lambda \Delta\lambda E_\lambda T_\lambda$
2. Monochromatic	I_λ(ergs cm^{-2} s^{-1})	$2.28 \times 10^{12} I_\lambda \lambda E_\lambda T_\lambda$
3. Normalized Continuum	$\frac{F_\lambda}{F_{5556}}, m_{5556}$	$7720 \frac{F_\lambda}{F_{5556}} \lambda \Delta\lambda E_\lambda T_\lambda 10^{-0.4 m_{5556}}$
4. Planck Function	T_{eff}(K), m_{5556}	$4.09x10^{22} \left(\frac{e^{\frac{25897}{T}} - 1}{e^{\frac{1.4388x10^8}{\lambda T}} - 1} \right) \Delta\lambda \frac{E_\lambda T_\lambda 10^{-0.4 m_{5556}}}{\lambda^4}$
5. Continuum	F_λ(ergs cm^{-2} s^{-1} hz^{-1})	$6.83x10^{30} \frac{F_\nu \Delta\lambda E_\lambda T_\lambda}{\lambda}$
6. Normalized Continuum	$\frac{F_\nu}{F_{\nu, 5556}}, m_{5556}$	$2.38x10^{11} \frac{F_\nu}{F_{\nu,5556}} \frac{\Delta\lambda E_\lambda T_\lambda}{\lambda} 10^{-0.4 m_{5556}}$
7. Power Law $\nu^{-\alpha}$	α, m_{5556}	$2.38x10^{11} \left(\frac{\lambda}{5556}\right)^{\alpha} \left(\frac{\Delta\lambda E_\lambda T_\lambda}{\lambda}\right) 10^{-0.4 m_{5556}}$

E_λ = (Net HST Reflectivity) x (FOS Efficiency at Wavelength λ (Å)). See Figure 1.1.3.
T_λ = Throughput of aperture at Wavelength λ (Å). See Figure 1.1.4.
$\Delta\lambda$ = Number of Angstroms per diode at Wavelength λ (Å). See Table 1.1.1.

Note that the relevant count rate to derive SNR per resolution element is N_λ (counts- sec^{-1} $diode^{-1}$). A resolution element is one diode, regardless of sub-stepping.

Table 1.2.2
Counts-sec^{-1}-diode^{-1} for representative spectral types at 15th magnitude.

Blue Detector								
Spectral Type	G130H (λ_{peak}=1600 Å)	G190H (λ_{peak}=2300 Å)	G270H (λ_{peak}=2650 Å)	G400H (λ_{peak}=3250 Å)	G570H (λ_{peak}=4600 Å)	G160L (λ_{peak}=2440 Å)	G650L (λ_{peak}=4000 Å)	PRISM (λ_{peak}=4000 Å)
B0V	2.1	8.0	16	15	2.0	28	18	1.8×10^2
A5V	1.5×10^{-3}	0.30	1.0	1.8	1.5	1.0	11	94
G2V	6.8×10^{-4}	3.0×10^{-3}	0.22	1.1	1.1	0.12	4.4	46
ν^{-1}	0.20	1.5	3.2	4.0	1.2	4.8	7.2	74
ν^{-2}	1.9×10^{-2}	0.60	1.5	2.4	1.0	2.2	5.2	53

Red Detector								
Disperser (λ_{peak})	G190H (λ_{peak}=2300 Å)	G270H (λ_{peak}=2650 Å)	G400H (λ_{peak}=3600 Å)	G570H (λ_{peak}=4600 Å)	G780H (λ_{peak}=6300 Å)	G160L (λ_{peak}=2400 Å)	G650L (λ_{peak}=4400 Å)	PRISM (λ_{peak}=4000 Å)
B0V	14	23	17	13	2.7	44	43	2.9×10^2
A5V	0.52	1.5	2.9	9.6	3.0	1.2	32	2.0×10^2
G2V	5.6×10^{-3}	0.32	2.2	7.2	3.8	0.18	11	1.2×10^2
ν^{-1}	2.6	4.4	6.0	7.6	4.0	8.0	23	1.6×10^2
ν^{-2}	1.1	2.2	4.0	6.4	4.8	3.4	18	1.3×10^2

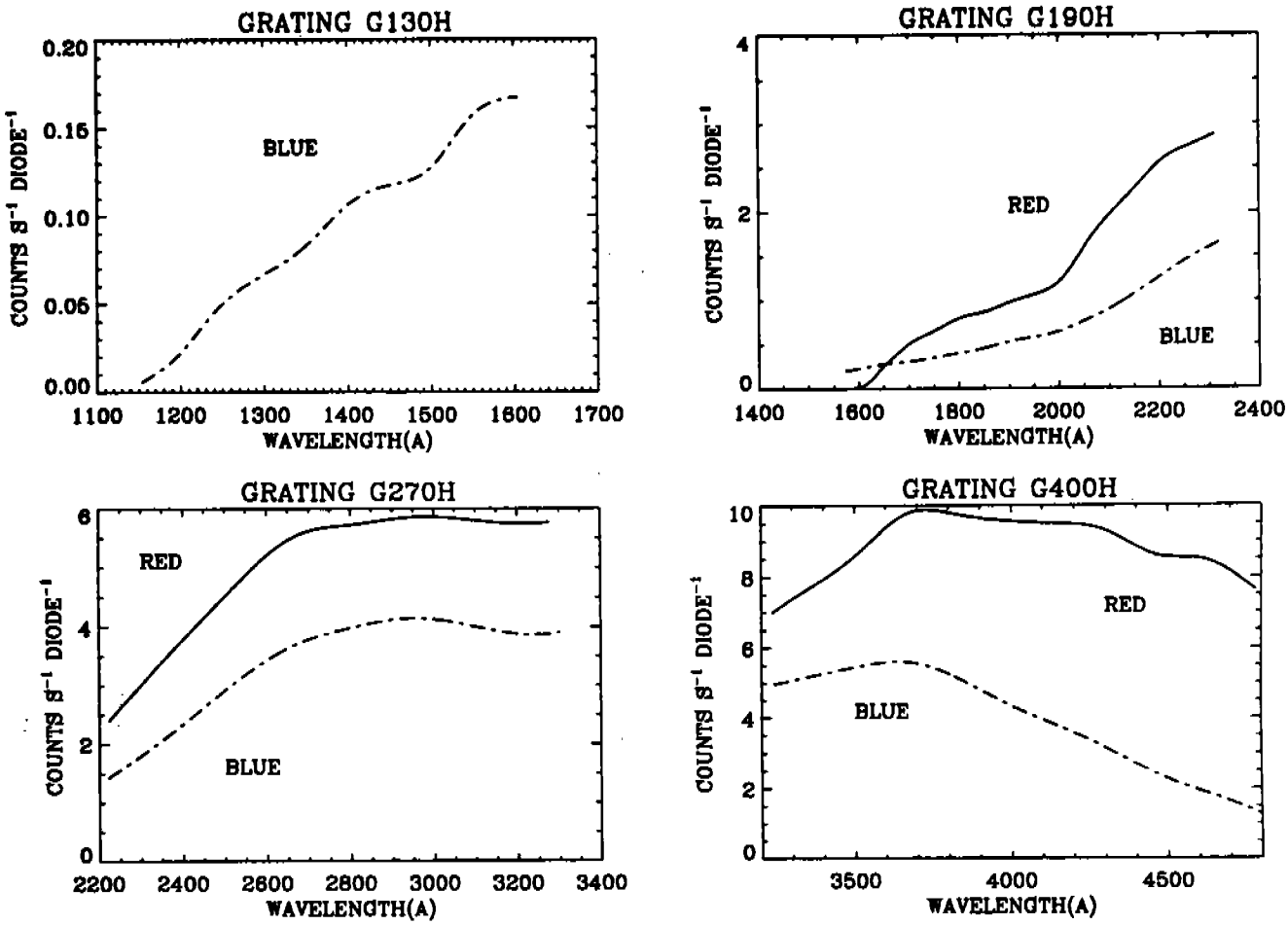

Figure 1.2.3: Detected counts-s^{-1}-diode^{-1} for input spectrum. $F_\lambda = 1 \times 10^{-14}$ erg-cm^{-2}-s^{-1}-Å^{-1} ($F_\lambda \propto \lambda^0$, or $F_\nu \propto \nu^{-2}$, with V=13.9) observed in the 4.3″ aperture.

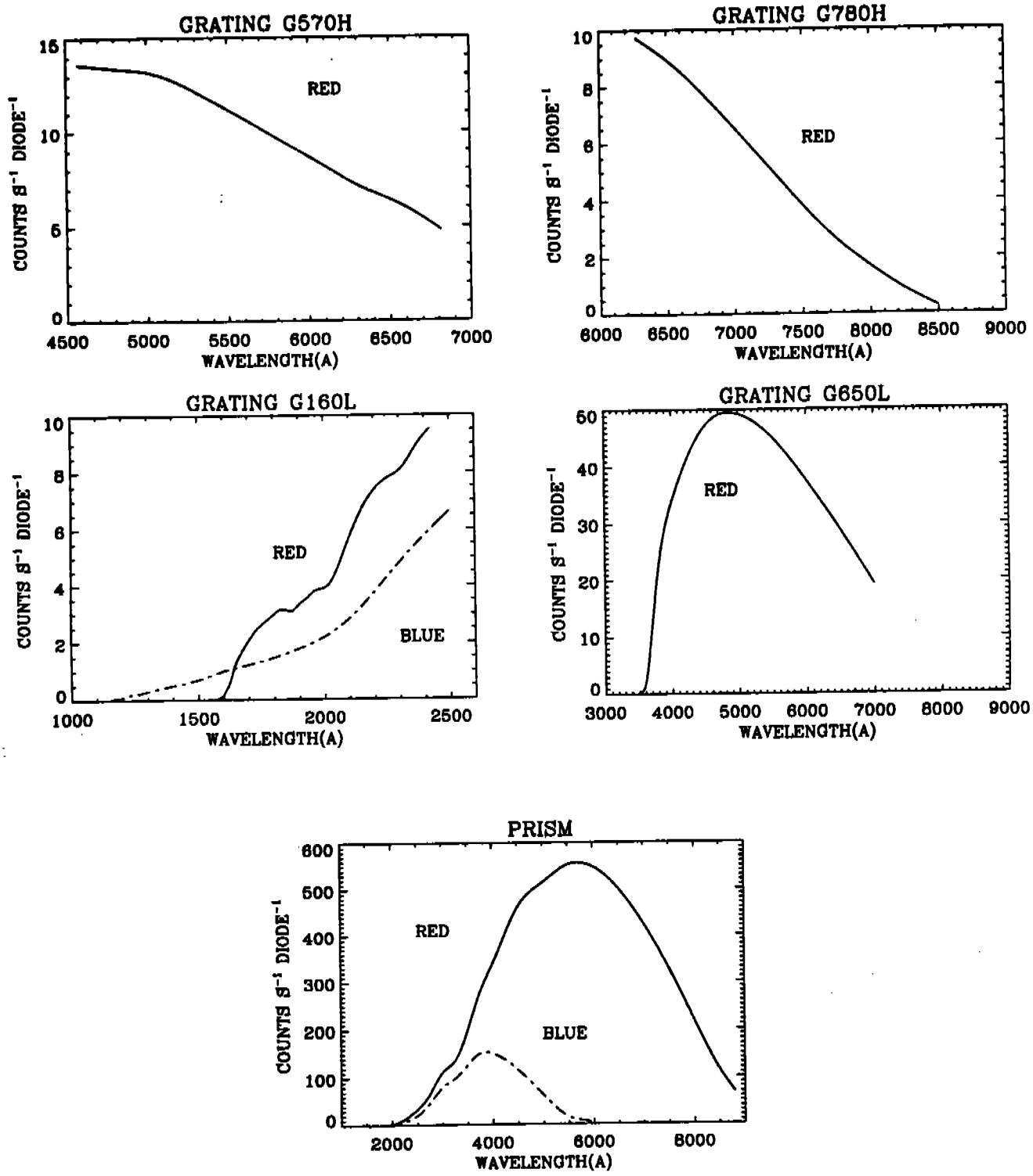

Figure 1.2.3 (*Continued*): Detected counts-s^{-1}-diode^{-1} for input spectrum. $F_\lambda = 1 \times 10^{-14}$ erg-cm^{-2}-s^{-1}-Å^{-1} ($F_\lambda \propto \lambda^0$, or $F_v \propto v^{-2}$, with V=13.9) observed in the 4.3″ aperture.

1.3 Brightness Limits

The Digicon detectors can be damaged by illumination from sources that are too bright. The brightness limit of the detectors have been translated into a limit of total counts detected in 512 diodes per 60 seconds – the overlight limit. If the overlight limit is exceeded in a 60 second exposure, the FOS automatically safes – *i.e.*, the FOS shuts its aperture door, places all wheels at their rest position, and stops operation. The overlight protection limit is 1.2×10^8 counts per minute integrated over the 512 diodes for the gratings and 12×10^6 counts per minute for the mirror. The visual magnitudes for unreddened stars of representative spectral types corresponding to this limiting count rate are given in Table 1.3.1 for all grating settings. The restrictions on target brightness are also found in the Bright Object Constraints Table of the Proposal Instructions (Table 5.15).

Table 1.3.1
Brightness Limits

Disperser/Mirror	Red Detector Brightness Limit				Blue Detector Brightness Limit			
	B0V	A5V	G2V	v^{-1}	B0V	A5V	G2V	v^{-1}
G130H	--	--	--	--	6.6	-2.0	-5.7	3.7
G190H	8.6	4.7	1.1	6.4	8.0	4.0	0.5	5.8
G270H	9.2	6.3	5.0	7.6	8.8	5.9	4.7	7.2
G400H	8.8	7.7	7.2	7.8	8.1	6.8	6.2	7.1
G570H	7.7	7.6	7.6	7.6	4.7	4.5	4.3	6.9
G780H	5.4	5.7	6.0	6.3	--	--	--	--
G160L	8.4	4.5	1.0	6.2	8.1	4.0	0.7	5.9
G650L	8.0	7.6	7.4	7.7	6.1	5.6	5.1	5.5
PRISM	10.1	8.5	8.2	9.0	9.6	7.5	6.8	8.2
MIRROR	12.8	11.2	10.8	11.6	12.4	10.0	9.3	10.7

1.4 Time Resolution

Spectra are taken with FOS by specifying either ACCUM, RAPID, or PERIOD mode on the Observation Summary Form when submitting an HST proposal. The manner that FOS data is taken depends on which of the three modes it is observed with.

FOS data is taken in a nested manner, with the smallest unit being livetime plus deadtime (see Appendix A for a full description of data taking). Standard spectra for the three

observing modes are taken by sub–stepping the diode array along the dispersion in the X direction, with steps one-quarter the diode width (12.5 micron, or 0.089″), and by scanning over 5 diodes in total to minimize the impact of dead diodes. A typical data taking sequence would divide the exposure time into twenty equal bins, and then perform the sequence of (livetime + deadtime), sub–stepped four times. That sequence would be performed 5 times, each sequence stepping to the next diode. As each of the 5 over–scanned spectra are obtained, they are added to the same memory locations of the previous spectra, so that over–scanning does not increase the amount of data. The data taking is then performed as (livetime + deadtime) × sub–stepping × over–scanning, or

$$(\mathrm{LT} + \mathrm{DT}) \times 4 \times 5.$$

1.4.1 ACCUM

FOS observations longer than a few minutes are time resolved. Spectra taken in a standard manner in ACCUM mode are read out at regular intervals. The red side (FOS/RD) is read out at $\leq$ 2 minute intervals, while the blue side is read out (FOS/BL) at $\leq$ 4 minute intervals. The standard output data for ACCUM mode preserves the time resolution in "multi–group" format. Each group of data is preceded by group parameters with information that can be used to calculate start time of the interval, plus a spectrum for each 2 minute (4 minute) interval of the observation. Each consecutive spectrum (group) is made up of the sum of all previous intervals of data. The last group of the data set contains the spectrum from the full exposure time of the observation.

1.4.2 RAPID

For objects needing higher time resolution, RAPID mode reads out FOS data at a rate set by the observer with the parameter READ-TIME. The shortest READ-TIME is 0.03 seconds. RAPID data is also in "multi–group" format. Each group contains group parameters with FOS related information followed by the spectrum for one time segment. (Of particular interest among the group parameters is FPKTTIME, which is used to derive the start time for each individual exposure, as given in Appendix A.)

READ-TIME is equal to livetime plus deadtime plus the time to read out FOS.

$$\mathrm{READTIME} = \mathrm{LT} + \mathrm{DT} + \text{Readout time}$$

The read–out time for FOS is dependent on the read-out rate, and on the amount of data to be read out, which is dependent on number of diodes (*i.e.*, the wavelength range) being observed, as well as on the sub–stepping. For the fastest READ-TIMEs, the rate of reading data can be stepped up from the default data rate of 32kHz to 1MHz, the wavelength region can be decreased, and sub–stepping set to 1. (The amount of data being taken by FOS must be decreased to achieve the fastest READ-TIME because a smaller amount of data can be read out in a faster time.) The data size, which cannot exceed 12,288, is given by

$$\text{Data size} = (\mathrm{NCHNLS} + \mathrm{MUL} - 1) \times \mathrm{SUBSTEP}$$

where NCHNLS is the number of diodes read out, MUL is the multiplicity, or the number of diodes that are over–scanned (usually 5) and SUB-STEP is the number of steps along the dispersion

(usually 4). The relation between number of diodes read out and wavelength coverage can be derived from Table 1.1.1. (Table 1.1.1 is accurate to within a few Ångstroms since it is based on data that was not corrected for the geomagnetically induced image drift, Kriss, Blair, & Davidsen 1991. See also Section 3.1 on wavelength calibrations.)

For a standard ACCUM exposure, the data size, which cannot exceed 12,288, is given by

$$\text{Data size} = (512 + 4) \times 4$$

$$\text{Data size} = 2,064$$

The read out time for spectral data is given by

$$\text{Readout time} = 0.0335 \times \text{INT}\left(\frac{\text{Data size}}{N}\right) \times \text{SUBSTEP seconds}$$

where INT(Data size/N) is the next largest integer corresponding to the ratio of Data size divided by 50 for the first packet, and divided by 61 for all subsequent packets. This equation is for data that is read out at the 32kHz data rate. If more than 20% of READ-TIME is spent reading out data, then the faster data rate is used, so that the read out time becomes

$$\text{Readout time} = 0.0028 \times \text{INT}\left(\frac{\text{Data size}}{N}\right) \times \text{SUBSTEP seconds}$$

When the faster data rate is in use, there is a limit of twenty minutes to the amount of contiguous data that can be recorded, due to the size of memory on the onboard tape recorder.

1.4.3 PERIOD

For objects that have a well known period, FOS data can be taken in PERIOD mode in such a way that the period is divided into BINS, where each bin has a duration of Δt = period/BINS. The period of the object is then given by the parameter CYCLE-TIME. The spectrum taken during the first segment of the period, Δt_1, is added into the first memory location. The spectrum taken during the second segment, Δt_2, is added to a contiguous memory location, and so on. The number of segments that a period can be divided into depends on the amount of data each spectrum contains, which depends on the number of sub-steps, whether or not the data is overscanned, and how large a wavelength region is to be read out. If the full range of diodes are read out, and the default observing parameters are used, 5 BINS of data can be stored. PERIOD mode data is single group, with a standard header followed by the spectra stored sequentially, where there are BINS spectra.

The data size, which cannot exceed 12,288, is given for PERIOD by

$$\text{Data size} = (\text{NCHNLS} + \text{MUL} - 1) \times \text{SUBSTEP} \times \text{BINS}$$

where BINS applies to PERIOD mode only. BINS is the number of time–segments to divide periodic data into. If the observer needs a larger number of BINS than 5, the wavelength range can be decreased, or the sub–stepping can be decreased to 2 or 1. (See Table 1.1.1 for relation between number of diodes [NCHNLS], and wavelength dispersion.)

1.5 Polarization

A Wollaston prism plus rotating waveplate can be introduced into the FOS to produce twin dispersed images of the slit in opposite senses of polarization at the detector (Allen and Angel 1982). Although there are two waveplates available, only waveplate B is currently recommended for use, and only in the wavelength region 1280–3310Å (Allen and Smith 1992). The geomagnetic image motion problem of the red Digicon precludes the use of the red side for polarimetry until after the on–orbit correction is applied in the fall of 1992. No polarimetry is anticipated after the Corrective Optics (COSTAR) installation because of strong instrumental polarization introduced, so that Cycle 3 is expected to be the last HST cycle for FOS polarimetry.

Only larger apertures (the effective $4.3'' \times 1.4''$ and possibly the $1.0''$ circular) have enough throughput to be useful for polarimetric observations of astronomical targets. Because the split spectra are slightly curved, small losses can occur even in these large apertures. The losses can vary because of changes of the position of the grating wheel, so that absolute fluxes are difficult to measure. However, the polarization measurements are not affected, since the grating remains fixed during one polarization observation.

The low dispersion gratings of FOS have slightly elongated images that significantly overfill the diode array when used with the (effective) $4.3'' \times 1.4''$ aperture. Because these losses negate much of the improvement in efficiency due to using the large aperture, only the high resolution gratings are recommended for polarimetry.

Although the "A" waveplate was designed to do well at Lyα λ 1216Å, the split spectra are not well separated by the "A" waveplate, so that the polarization at Lyα cannot be observed. Linear polarization observations in the wavelength range should use the "B" waveplate and gratings G130H, G190H, and G270H.

In summation: 1) Only blue side polarimetry can be done until the on–orbit fix to the geomagnetically induced image drift is in place in the fall of 1992. After that, both blue side and red side polarimetry will be available. 2) Only high resolution gratings are recommended for polarimetry. 3) For observations in the UV, use the B waveplate. 4) Polarimetry will not be available after COSTAR is deployed.

The sensitivity of the polarizer depends both upon its throughput efficiency and its modulation efficiency (η_{thr} and η_{mod}, both given in Figure 1.5.1). The modulation efficiency can be calculated from the retardation by

$$\eta_{mod}(linear) = (1 - \cos\Delta)/2$$

$$\eta_{mod}(circular) = \sin\Delta$$

The detector can only observe one of the two spectra produced by the polarizer so that another factor of two loss in practical throughput occurs. The count rate is given by

$$\text{Count rate(pol)} = \text{Count rate(FOS)} \times \eta_{mod} \times \eta_{thr} \times 0.5$$

1.6 FOS Noise and Dynamic Range

The minimum detectable source levels are set by instrumental background, while the maximum accurately measurable source levels are determined by the response times of the FOS electronics.

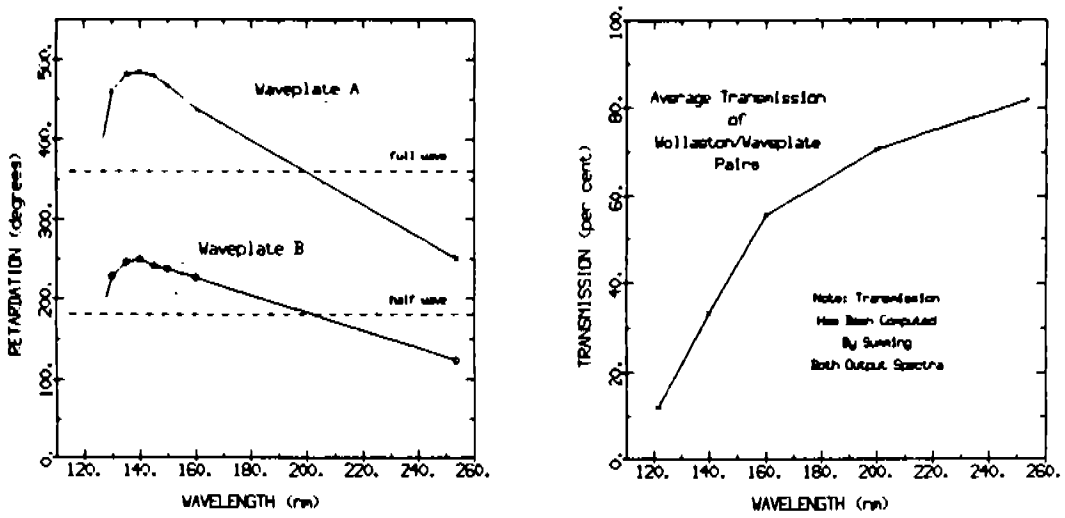

Figure 1.5.1: FOS waveplate retardation (left) and polarimeter transmission (Allen & Angel, 1982).

When the FOS is operating outside of the South Atlantic Anomaly, the average dark count rate is roughly 0.01 counts s^{-1} $diode^{-1}$ for the red detector and 0.007 counts s^{-1} $diode^{-1}$ for the blue detector (Rosenblatt *et al.* 1992). However, Rosenblatt *et al.* note that the background count rate varies with geomagnetic latitude such that higher rates are observed at higher latitudes. The detected counts s^{-1} $diode^{-1}$ plots given in Figure 1.2.3 for an input spectrum with constant flux of $F_\lambda = 1 \times 10^{-14}$ erg cm^{-2} s^{-1} $Å^{-1}$ can be compared with the observed dark count rate to determine the limiting magnitude for FOS. For example, for an object observed on the red side at 2600Å, an incident flux of $F_\lambda = 1.3 \times 10^{-17}$ erg cm^{-2} s^{-1} $Å^{-1}$ would produce a count rate comparable to the red side dark rate. For an object observed on the blue side at 2600Å, an incident flux of $F_\lambda = 3.0 \times 10^{-17}$ erg cm^{-2} s^{-1} $Å^{-1}$ would produce a count rate comparable to the blue side dark rate.

In the other extreme, for incident count rates higher than approximately 100,000 counts s^{-1} $diode^{-1}$, the observed output count rate does not have an accurate relation with the true input count rate. Figure 1.6.1 shows a preliminary determination of the relation between true count rate and observed count rate, as measured by Lindler and Bohlin (1986, measured for high count rates for the red side only). For observed count rates above 100,000 counts s^{-1} $diode^{-1}$, the correction exceeds a factor of 2 and the accuracy decreases drastically. By the time a true count rate of 200,000 counts s^{-1} $diode^{-1}$ is reached, the error in the correction to the true rate is of order 50%.

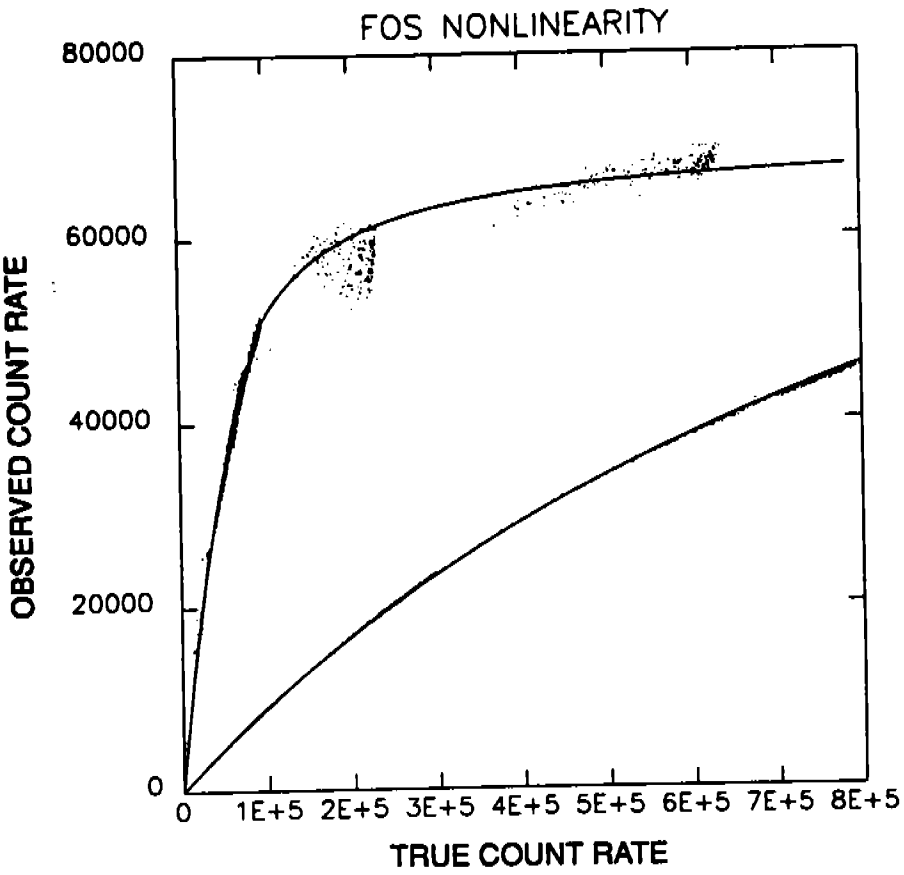

Figure 1.6.1: Measured count rate versus true count rate (D. Lindler and R. Bohlin, 1986). The lower curve is a plot of the upper curve expanded by 10 in the x-direction.

2.0 OBSERVING MODES

2.1 Acquiring the Target: ACQ

The HST pointing is accurate and reliable. To demonstrate the accuracy of the HST pointing, Figure 2.1.0 shows the slews performed after FOS target acquisition to center the target in the science aperture for observations taken after early 1991. The position $V_2 = 0.0$ and $V_3 = 0.0$ in Figure 2.1.0 corresponds to perfect initial pointing. Figure 2.1.0 shows that, using positions derived from GASP, about 75% of the blind pointings fall within $1''$ of the aperture center. However, onboard target acquisition is still necessary with FOS for centering the target in the science aperture.

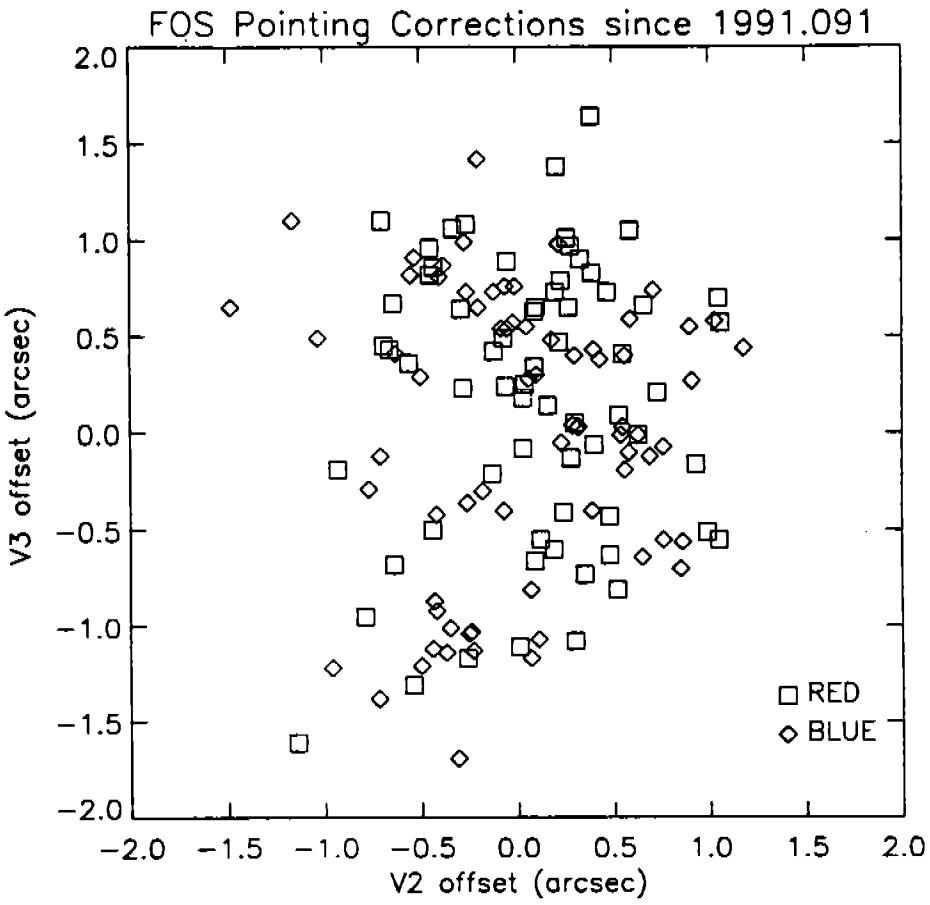

Figure 2.1.0: Slews performed after FOS target acquisition to center the target in the science aperture. The average red side offset is: V2=$0.08'' \pm 0.06''$, V3=$0.18'' \pm 0.09''$. The average blue side offset is: V2=$0.01'' \pm 0.07''$, V3=$-0.01'' \pm 0.09''$.

An interactive acquisition (set with the SPECIAL REQUIREMENT , INT ACQ) and three onboard acquisition modes (ACQ/BINARY, ACQ/PEAK, and ACQ/FIRMWARE) are described below. During an onboard acquisition, the telescope slews to the object, performs the acquisition, calculates the small offset required to center the target in a science aperture, makes the offset, and then begins the science exposure. In contrast, during an interactive acquisition there must be a real time contact with HST, and the observer must be present at the ST ScI to interpret the image. Because of the considerable possibility of real time confusion when looking at an FOS white light picture, we believe that in nearly all cases a WF/PC assisted target acquisition will be a better scientific choice than an early FOS acquisition (ACQ). However, ACQ does also provide an important means of verifying, after the fact, where the FOS aperture was positioned on the target during a science exposure for both WF/PC early acquisition and for onboard acquisitions of targets in complex fields.

The FOS acquisition aperture is $4.3'' \times 4.3''$ square. In order to have a 95% chance of placing a star in this aperture, the star *must* have an RMS positional error with respect to the guide stars of less than $1.0''$. The FOS finds the star by deflecting its electronic image along the diode array and perpendicular to the diode array. The acquisition aperture is 12 diodes wide and 3 diodes high, as illustrated in Figure 1.1.1. Because the diode is rectangular, with the X direction smaller than the Y direction ($0.36'' \times 1.43''$), the two directions are treated differently in target acquisition.

Additional acquisitions are not necessary when switching from the red side to the blue side, since the aperture positions are accurately known. Once a target has been acquired into a large science and observed with one detector, a slew can be performed to place the target directly into the aperture for the other detector. Such slews would not be accurate enough to place objects in the (effective) $0.25'' \times 1.4''$ slit or the $0.3''$ aperture, however. (See the exposure logsheet lines 3.0 through 4.3 in Appendix E.) Note that when using acquisitions on just one side of FOS for acquiring into both sides, the exposure logsheet lines must be tied together by SPECIAL REQUIREMENTS of the form ONBOARD ACQ FOR 4-4.3 and with SEQ 3-4.3 NO GAP (Appendix E).

2.1.1 INT ACQ

The mode ACQ, when used with the SPECIAL REQUIREMENT, INT ACQ FOR, maps the acquisition aperture and sends the image to the ground in real time. The apparent elongation of stars in the y-direction caused by the shape of the diodes ($0.36'' \times 1.43''$) is removed on the ground by multiplying the picture by an appropriate matrix. After the picture has been restored, the astronomer measures the position of the target on the image. The small offset required to move the target to the center of one of the science apertures is calculated and uplinked to the telescope; after the slew is performed the science observations begin.

ACQ can also be used after another type of acquisition to provide a picture which shows where HST is pointed in FOS detector coordinates. The Exposure Logsheets provide an example (lines 5 - 8, Appendix E) of an ACQ/BINARY of an offset star followed by an offset onto the nucleus of M81. In this example, after the science observation is made, a (white light) picture of the aperture is taken by using ACQ to verify the aperture position.

2.1.2 ACQ/BINARY

During an ACQ/BINARY, the camera mirror reimages the FOS focal plane onto the Digicon. ACQ/BINARY first finds the number of stars in the $4.3'' \times 4.3''$ acquisition aperture by integrating at three different positions in the y-direction. The program locates the target in one of the three strips, measures its count rate, and locates the target in the X direction. The algorithm then positions the target on the Y–edge of the diode array by deflecting the image across the diode array through a geometrically decreasing sequence of Y–deflections until the observed count rate from the star is half that when the object is fully positioned on the diode array. ACQ/BINARY is the preferred acquisition mode for point sources.

Although ACQ/BINARY is designed to obtain the Nth brightest star in a crowded field by setting the optional parameter NTHSTAR, acquisitions in crowded fields are not recommended given the current PSF.

There should be about 300 counts in the peak pixel for each y-step that is on-target for Binary Search to succeed. If the number of counts in the peak is significantly larger than 300, the tolerances for when the target is half in the aperture become very small since they are based on $\sqrt{N}$ statistics. With the image drift due to the poor magnetic shielding and due to spacecraft jitter, the Binary Search can fail if the tolerances are too small. Typical centering error after Binary Search is $\lesssim 0.2''$.

A target must lie within the range of counts specified by the Optional Parameters BRIGHT and FAINT. We recommended that BRIGHT and FAINT be set to allow for targets 10 times brighter and 5 times fainter than expected. Since the maximum number of y-steps in Binary Search is 11, the default values for the parameters are BRIGHT = 300 × 11 × 10 = 33,000 and FAINT = 300 × 11/5 = 660. The FAINT limit is particularly important since the wings of the PSF can appear as independent targets if the FAINT limit is set too low. When more than 5 independent targets are detected per y–step, the Binary Search fails. FAINT should be set at about 20% of the target peak to avoid the wings of the PSF.

Examples of an ACQ/BINARY on an offset star followed by an FOS observation of the target star is given on lines 1 and 2 of the sample logsheets (Appendix E).

2.1.3 ACQ/PEAK

During ACQ/PEAK the telescope slews and integrates at a series of positions on the sky with a science aperture in place. At the end of the slew sequence the telescope is returned to the position with the most counts. In the case of an ACQ/PEAK into a barred aperture, or when using the Optional Parameter TYPE=DOWN, the telescope is returned to the position with the fewest counts. ACQ/PEAK is a relatively inefficient acquisition because a minimum of $\sim$ 42 seconds per dwell is required for the telescope to perform the required small angle maneuvers.

This mode is to be used to acquire objects too bright to acquire with the camera mirror in place, to center targets in the smallest apertures, and to position bright stellar sources on the bars of the occulting apertures in order to observe any surrounding nebulosity. Examples of ACQ/PEAK are given on lines 9 though 10.6 of the sample Exposure Logsheets (Appendix E).

Because the $0.25'' \times 2.0''$ slit maximizes collecting area with little degradation of the spectral resolution, this slit will commonly be used for science observations. Thus, ACQ/PEAK

into the $0.25'' \times 2.0''$ slit will often follow ACQ/BINARY. To acquire objects into the slit, first use a normal ACQ/BINARY acquisition, followed by an ACQ/PEAK into the slit using the SPECIAL REQUIREMENT SPATIAL SCAN. The ACQ/PEAK must have a high number of counts to place the target in the center of the slit ($\approx$ 12000). Coincidentally, the exposure time used for ACQ/PEAK into the slit is the same as the exposure time used in ACQ/BINARY (Table 2.1.2 below). An example is given in logsheet lines 3 through 4.3 (Appendix E).

Note that count rates must not exceed the safety limits for the mirror or the grating selected (see Table 1.3.1 and Table 2.1.1).

Critical ACQ/PEAK for centering into the small ($0.3''$ and less) apertures should be performed after ACQ/BINARY acquisitions (for faint objects) and after non-critical ACQ/PEAK (for bright objects). A critical ACQ/PEAK requires relatively long exposure times (see Section 2.1.6) and spacing between dwells of order *D/5,* where *D* is the diameter of the Peak Up aperture. The non-critical ACQ/PEAK requires shorter exposure time and spacing between dwells of order *D/2.*

The pattern of moves on the sky can be specified by the observer and can, for example, be either a raster scan or a linear scan in the Y direction, such as is used for acquisition into the $0.25'' \times 2.0''$ aperture. For a user–defined slew sequence into a science aperture, the SPECIAL REQUIREMENT column should state SPATIAL SCAN and a SPATIAL SCAN form must be included. A common example, ACQ/PEAK into the $0.25'' \times 2.0''$ slit, is given in the examples below under ACQ/PEAK.

2.1.4 ACQ/FIRMWARE

ACQ/FIRMWARE is an engineering mode which maps the camera-mirror image of the aperture in X and Y with small, selectable Y increments. The FOS microprocessor filters the aperture map and then finds the y-positions of the peaks by fitting triangles through the data. Firmware is less efficient than Binary Search, and fails if more than one object is found within the range of counts set by the observer (BRIGHT and FAINT).

2.1.5 WF/PC Assisted Target Acquisition

We recommend using WF/PC assisted target acquisition when there will be more than two stars in the $4.3''$ acquisition aperture or when there will be intensity variations across the acquisition aperture which are larger than a few percent of the mean background intensity. A WF/PC assisted target acquisition is accomplished by first measuring the positions of the target and an offset star in a WF/PC image and then (at least 2 months later) acquiring the offset star with ACQ/BINARY and then offsetting the FOS aperture onto the target. Although the position of the target can be measured very accurately in the WF/PC image, the offset star is needed because there is only about a 30% chance that the same guide stars will be in the Fine Guidance Sensors (FGS) when the subsequent FOS observations are made. With new guide stars, the 1σ uncertainty in any position is $0.3''$. Error in position angle also limits the size of the offset slew to $2.7'$ for acquiring objects for the smallest ($0.1''$ pair) FOS aperture. Since the Wide Field Camera is $2.7'$ on a side, it is unlikely that an offset slew of more than $2.7'$ will be needed. (Note that offsets larger than $30''$ should be discussed with the User Support Branch.)

The first step in a WF/PC assisted target acquisition is to use a SPECIAL REQUIREMENT on the Exposure Logsheets to specify the exposure as an EARLY ACQ which must be taken

at least two months before the FOS observations (see lines 5 through 8 on the exposure logsheet in Appendix E). The camera (WFC or PC), exposure time, filter, and centering of the target in the image should be chosen such that the picture will show both the target and an isolated (no other star within 6″) offset star which is brighter than $m_V = 20$ and more than 1 magnitude brighter than the background (magnitudes per square arcsecond). In order to insure that an appropriate offset star will be in the WF/PC image, the centering of the target in the WFC or PC field should be chosen by measuring a plate or CCD image. The Target List should provide the offset star with nominal coordinates and with position given as TBD-EARLY. (See example lines 4 and 5 on the Target List.) The Target List also should list the position of the offset star as RA-OFF, DEC-OFF, and FROM the target. Alternatively, the offsets can be given as XI-OFF and ETA-OFF, see the Phase II Proposal Instructions Section 5.1.4.3 on Positional Offsets.

After the exposure has been taken and the data has been received, the next step is to get the picture onto an image display so you can i), choose an offset star, ii) measure its right ascension and declination, and iii) measure the right ascension and declination of the target relative to the offset star. There will be an STSDAS program available to extract pointing and roll angle information from the WF/PC header and convert WF/PC pixels to right ascension and declination. If this program is not available, you will need to patch your WF/PC image into the Guide Star Catalog reference frame. Based on your choice of an offset star, the ST ScI will choose a pair of guide stars for the FOS observations which will stay in the "pickles" during the move from the offset star to the target. The probability that a suitable pair of guide stars can be found increases as the separation of the offset star and the target decreases. So, choose the offset star as close as possible to the target (but not so close as to violate the background rule in the preceding paragraph). The final step is to send the position of the offset star and the positional offsets to the ST ScI to update the proposal information for your succeeding FOS observations.

2.1.6 Examples

The following section gives examples for acquiring different types of astronomical objects based on the strengths and weaknesses of the various target acquisition methods.

Single Stars

Stars with visual magnitudes brighter than about 13^{th} are too bright for FOS acquisitions with the camera mirror, and observations of objects that bright will safe the instrument. The exact limit depends on the spectral type of the star and on the detector as shown in Table 2.1.1 below.

Table 2.1.1
FOS Visual Magnitude Limits with Camera Mirror

	O7V	B0 V	B3 V	A1 V	A5 V	G2 V	K0 III	ν^{-1}
Red Side Limit	13.0	12.8	12.2	11.4	11.2	10.8	10.5	11.6
Blue Side Limit	12.5	12.4	11.6	10.3	10.0	9.3	8.5	10.7

Stars which are too bright for ACQ/BINARY can be acquired by using ACQ/PEAK with one of the high dispersion gratings instead of the camera mirror (see lines 10.3 though 10.6 on the Exposure Logsheets in Appendix E). If the visual magnitude of a single star or point source is fainter than limits given in Table 2.1.1 above, use ACQ/BINARY for the acquisition.

Stars Projected on Bright Backgrounds

ACQ/BINARY can successfully find a star projected on a uniform background provided the target acquisition integration time is long enough to give $\sim$ 300 peak counts from the star and the star is at least a magnitude brighter than the background surface brightness in magnitudes per square arcsecond. If star and the background vary by less than 1 magnitude, the star can still be acquired with ACQ/BINARY by increasing the integration time. Alternatively, the acquisition can be accomplished by using a WF/PC assisted acquisition.

A different problem arises when the background varies across the acquisition aperture. Because the logic in the ACQ/BINARY program drives the star to the edge of the diode array by finding the position which gives half the maximum number of counts, any change in the background in the y-direction will bias the derived y-position of the star. Simulations of acquisitions of stars projected onto bright galaxies such as NGC 3379 show that the shot noise in the star will determine the accuracy (rather than the variable background), provided the star is at least $15''$ from the center of the galaxy. If in doubt, consult with the Institute staff, who will be able to simulate acquisitions for a reasonable number of cases. If there is any doubt about the success of ACQ/BINARY, you should plan a WF/PC assisted acquisition.

Diffuse Sources and Complex Fields

The FOS onboard acquisition methods were designed to acquire point sources. Consequently, diffuse sources and complex fields must be observed by first acquiring a star and then offsetting to the desired position in the source. The most accurate positioning of the FOS aperture on the source will be accomplished by using a WF/PC assisted target acquisition. In many programs, the interesting positions in the source will be chosen on the basis of WF/PC images. If the imaging program is planned as described in the section on WF/PC assisted TAs, the science images can be used for the acquisition.

Nebulosity Around Bright Point Sources

The optimal FOS aperture position for a bright point source surrounded by a nebulosity will depend on the distribution and brightness of the nebulosity relative to the point source. If high spatial resolution pictures show that the nebulosity has scale length of a few tenths of an arcsecond and is relatively symmetrical around the source, the signal-to-noise ratio may be maximized by placing the stellar source on the occulting bar of one of the occulting apertures and simultaneously observing the nebulosity on both sides of the occulting bar. When using this approach, you should first use Binary Search to position the source near the center of the occulting aperture. The second step is to use a Peak Down in the y-direction to position the stellar source on the occulting bar. An example is given in lines 11, 12, and 13 of the Exposure Logsheet (Appendix E).

If high resolution images show that the nebulosity is rather asymmetrical, the best approach may be to observe the nebulosity with one of the small circular apertures. In that

case the bright stellar source should be acquired with Binary Search followed by an offset onto the nebulosity.

ACQ/PEAK

The two examples discussed are the acquisition of a planetary object, where an area of sky larger than the TA aperture ($4.3'' \times 4.3''$) may have to be searched, and the acquisition of an object too bright to acquire with **ACQ/BINARY**. Both examples require use of a Scan Parameter Form since the standard square (**SEARCH-SIZE=N**) raster pattern is not optimal. The **SPATIAL SCAN** must be specified in the **SPECIAL REQUIREMENTS** column of the Exposure Logsheet for these cases. The Scan Parameter forms follow the Exposure Logsheet. The examples are written up on lines 9 through 10.6 and the Scan parameter forms are included following the Exposure Logsheet (Appendix E).

By using the target acquisition aperture, an effective aperture of size $4.3'' \times 1.4''$ (the diode height times the aperture width) is available and an area of $8.6'' \times 8.6''$ can be searched. The first two steps of the **ACQ/PEAK** are to perform a 2×6 dwell pattern with the (effective) $4.3'' \times 1.4''$ aperture followed by a 6×2 dwell pattern using the $1.0''$ aperture. These observations are shown on lines 9 and 10 of the exposure logsheet and on the Scan Parameter form. The third step of the **ACQ/PEAK** depends on the exact nature of the science to be done. One example is for an object to be centered into the $1.0''$ aperture by performing a non-critical **ACQ/PEAK** into the $0.5''$ aperture (line 10.1 on the Exposure Logsheet in Appendix E).

The most time efficient way to acquire a bright target with the FOS is again to use the (effective) $4.3'' \times 1.4''$ aperture in a 1×3 dwell pattern, followed by a 6×2 dwell pattern into a $1.0''$ aperture. The third step depends on the science to be done. As with the example given above, for an object to be centered into the $1.0''$ aperture, a non-critical **ACQ/PEAK** can be performed into the $0.5''$ aperture. These observations are shown on lines 10.3 through 10.6 on the Exposure Logsheet. The Scan Parameter forms follow the Exposure Logsheet.

2.1.7 Acquisition Exposure Times

There should be about 300 counts in the peak of each y-step of an **ACQ/BINARY** exposure. The maximum number of y-steps which can be taken during **ACQ/BINARY** is 11. Table 2.1.2 summarizes the total exposure time for an **ACQ/BINARY**, *i.e.* the time per y-step multiplied by 11, for various types of stars. *The exposure times in Table 2.1.2, scaled to the magnitude of the target, are the times which should be entered in the Exposure Logsheets.* There is a minimum integration time that can be entered on the exposure logsheet (constrained by the FOS livetime limit), given in Table 2.1.3. If the exposure time must be larger than that calculated from Table 2.1.2 to accommodate the minimum time, the values for the optional parameters **BRIGHT** and **FAINT** must be set to reflect the total number of counts expected.

$$\text{BRIGHT} = 33,000 \times \frac{\text{TIME}_{\text{Table 2.1.3}}}{\text{TIME}_{\text{Table 2.1.2}}}$$

$$\text{FAINT} = 660 \times \frac{\text{TIME}_{\text{Table 2.1.3}}}{\text{TIME}_{\text{Table 2.1.2}}}$$

Table 2.1.2
Total Exposure Times for FOS Firmware for 15^{th} Magnitude Objects Unreddened

Red Side				
Flux	Time ACQ/BINARY[1] ACQ/PEAK into slit[2]	Time ACQ/FIRMWARE[1]	Time ACQ/PEAK[3] Mirror	Time ACQ/PEAK[3] G780H
K0 III	8.9	12.9	0.34	1.8
G2 V	6.9	10.0	0.26	2.1
A5 V	4.9	7.1	0.19	3.0
A1 V	4.1	6.0	0.15	3.0
B3 V	1.8	2.6	0.068	3.2
B0 V	1.1	1.6	0.040	3.5
O7 V	0.90	1.3	0.034	3.0
ν^{-1}	3.3	4.8	0.12	1.6
ν^{-2}	4.6	6.7	0.17	1.4

Blue Side				
Flux	ACQ/BINARY[1] ACQ/PEAK into slit[2]	ACQ/FIRMWARE[1]	ACQ/PEAK[3] Mirror	ACQ/PEAK[3] Prism
K0 III	58.0	84.0	2.2	2.3
G2 V	28.0	41.0	1.1	1.1
A5 V	14.0	21.0	0.54	0.59
A1 V	11.0	16.0	0.41	0.44
B3 V	3.3	4.8	0.13	0.15
B0 V	1.6	2.3	0.060	0.082
O7 V	1.4	2.0	0.052	0.068
ν^{-1}	7.3	11.0	0.28	0.29
ν^{-2}	13.0	19.0	0.48	0.48

Note: Exposure time must be multiplied by $10^{0.4(V-15)}$.
[1] Optimal exposure times for ACQ/BINARY and ACQ/FIRMWARE are calculated to detect 300 peak counts in the peak pixel of the target.
[2] ACQ/PEAK into the (effective) $0.25'' \times 1.4''$ slit requires 12000 total counts, which can be obtained in the same amount of exposure time as used for ACQ/BINARY.
[3] Exposure times for ACQ/PEAK into all apertures excluding the slit are calculated to detect 1000 total counts for non-critical acquisitions. For critical centering into small apertures, multiply the exposure times by a factor of 10. **Note that the exposure time for ACQ/PEAK must be multiplied by the inverse throughput of the aperture used (T_λ, see Figure 1.2.2).** Although the exact factor depends on the input spectrum, the approximate multiplicative factors are 1.5 for the $1.0''$ apertures, 2.5 for the $0.5''$ apertures, and 4.0 for the $0.3''$ aperture.

For example, for a red side acquisition of a 12^{th} magnitude offset K0III star, 0.55s is the exposure time derived from Table 2.1.2, but the minimum exposure time is 0.66s. The default values of BRIGHT and FAINT must then be multiplied by the factor 0.66/0.55 = 1.2, so that BRIGHT = 39,600 and FAINT = 800.

The peak-up exposure times in Table 2.1.2 are calculated to produce 1000 counts in the peak of the target image, which is the number of counts recommended for the non-critical ACQ/PEAK described above. The ACQ/PEAK sensitivity has considerable wavelength and aperture size dependence. The critical ACQ/PEAK into small apertures requires 10,000 counts total to achieve a centering error which corresponds to a signal loss of less than about 2%. For critical Peak Up, the values in Table 2.1.2 relating to peak up must then be multiplied by a factor of 10. Note that times for Peak Up into the (effective) $0.25'' \times 1.4''$ slit are the same as times for ACQ/BINARY

The times in Table 2.1.2 do not include the overhead involved in the initial setup of parameters or the analysis time, since that overhead should not be included on the Exposure Logsheet specifications.

Table 2.1.3
Minimum Exposure Times to be Entered in Exposure Logsheets

ACQ/BINARY	0.66 sec
ACQ/FIRMWARE	0.96 sec
ACQ/PEAK	0.003 sec
ACQ	3.84 sec

2.2 Taking Spectra: ACCUM and RAPID

Spectropolarimetry: STEP-PATT = POLSCAN

Example of exposure logsheets are included for ACCUM mode (see lines 3.0 though 4.3 in Appendix E) and RAPID mode (see lines 11.0 through 13.0).

In RAPID mode, when a wavelength range is specified, that range will be used, whether or not there is room in memory for a larger region. Therefore, specifying a wavelength range is not a good idea unless absolutely necessary because it restricts the wavelength region that is read out. The full wavelength region is often useful. For example, the background can be determined directly from the diode array for gratings G130H, G160L, and G190H. The diodes below the lowest wavelength, given in Table 1.1.1, can be used to average the actual background rate. Also, the zero order can be monitored for G160L if all diodes are read out. However, if the observer needs a specific wavelength range, that range can be specified in column 8 of the Phase II exposure logsheet. Otherwise, the largest possible wavelength range will be automatically observed that is compatible with the READ-TIME requested.

The use of STEP-PATT = POLSCAN is demonstrated in the exposure logsheet lines 14.0 through 15.0.

3.0 INSTRUMENT PERFORMANCE AND CALIBRATIONS

3.1 Wavelength Calibrations

The wavelength calibrations on the dwarf emission line star AU Mic, which are corrected for image drift, are used to produce a measurement of the offsets in the wavelength scale between the internal calibration lamp and a known external point source (Kriss, Blair, & Davidsen 1992). On the red side, the mean offset between internal and external source is $+0.176 \pm 0.105$ diodes. On the blue side, the mean offset is -0.102 ± 0.100 diodes. These offsets are not included in the pipeline reduction wavelength calibration. With the observed dispersion reported by Kriss, Blair, & Davidsen, velocity measurements based on single lines in FOS spectra have a limiting accuracy of roughly 20 km s^{-1} if simultaneous wavelength calibrations are made. If simultaneous wavelength calibrations are not made, the non-repeatability in the positioning of the filter–grating wheel will dominate the errors in the wavelength scale.

3.2 Absolute Photometry

The absolute photometric calibration has been performed by observing the standard stars G191B2B (WD0501+527), BD+28D4211, BD+75D325, HZ–44, and BD+33D2642 several times in the large (effectively $4.3'' \times 1.4''$) aperture. The blue side calibrations of the G130H, G190H, G270H, G400H, G160L gratings, and the prism, all show an overall degradation of sensitivity of about 10% per year. The red side calibrations of the G190H, G270H, G400H, G570H, G780H, G160L, G650L gratings, and the prism, show sensitivity stable to within 5%, except in the region between 1800Å and 2100Å, where a trough is developing at the rate of up to 15% per year.

3.3 Flat Fields

Observations of two white dwarfs (G191–B2B and KPD 0005+5106) were made to produce spectral flat fields for the principal FOS grating and detector combinations. Results of these tests are reported in Anderson (1992). The blue side flat fields display a typical standard deviation in the flats about their mean value of unity of the order of 1%. However, the red side is more problematical, exhibiting strong granularity in the G160L and the G190H gratings, and to a lesser extent in the G270H grating. The granularity has shown an increase between the first flat fields taken in October of 1990, and later flat fields taken in early 1992. The flat field of the large aperture (effectively $4.3'' \times 1.4''$) differs from the flat field of the other, smaller apertures. The red side spectral flat field will be monitored on a bi-monthly basis as part of the Cycle 2 calibration program to track any further changes in the red side flat fields. Because of the difference between the flat fields in the large aperture versus the smaller apertures, they will be taken in both the large aperture and in the slit (effectively $0.25'' \times 1.4''$). Figures 3.3.1, 3.3.2, and 3.3.3 show the data used to produce the red side flat fields for the G160L, the G190H, and the G270H gratings, respectively. The data taken in October of 1990 in these figures have been multiplied by a throughput factor of 1.6 because

they were taken in the 1.0″ aperture. The blue side and red side flat fields for G190H are shown in Figures 3.3.4 and 3.3.5, respectively.

Red side data taken after January 1992 can be flat fielded with the data taken closest in time to the observation. The STSDAS package getreffile will refer the user to the appropriate flat field. Because getreffile refers to the Calibration Data Base System (CDBS) for temporal information, the package is available only at ST ScI. For help with this package, observers can send requests to analysis@stsci.edu and ask that getreffile be run for the appropriate data set. Red side data taken between October 1990 and January 1992 will be difficult to flat field because of the lack of time–dependent flat fields available between 1990 and 1992.

3.4 Sky Lines

The lines of Ly$\alpha\lambda$1216. and OI λ1304 appear regularly in FOS spectra, with a width given by the size of the aperture (see Table 1.1.3). Occasionally, when observing on the daylight side of the orbit, the additional sky line of OII λ2470 can also be seen.

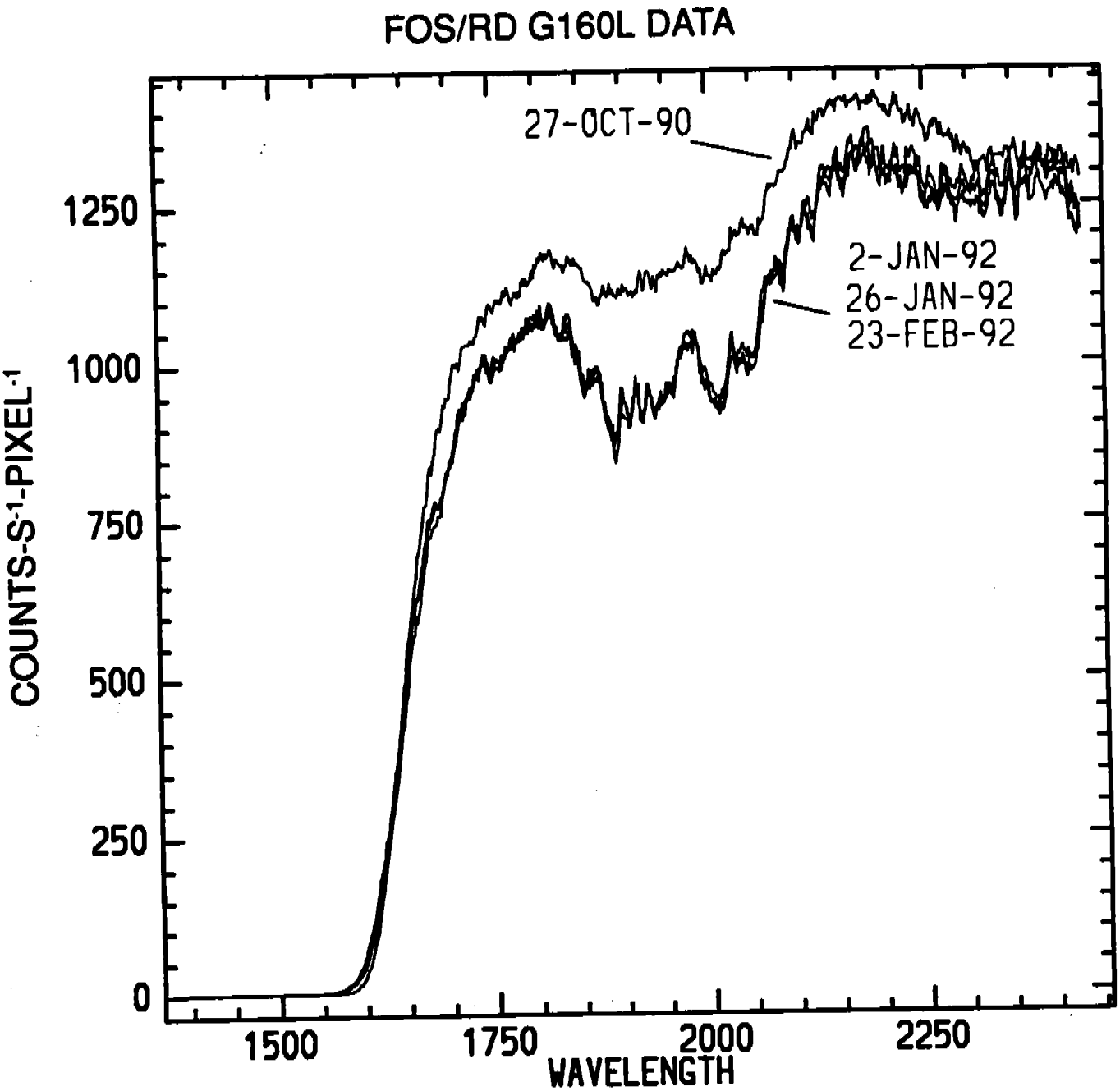

Figure 3.3.1: Redside G160L Data of target G191-B2B from which the Flat Fields are produced.

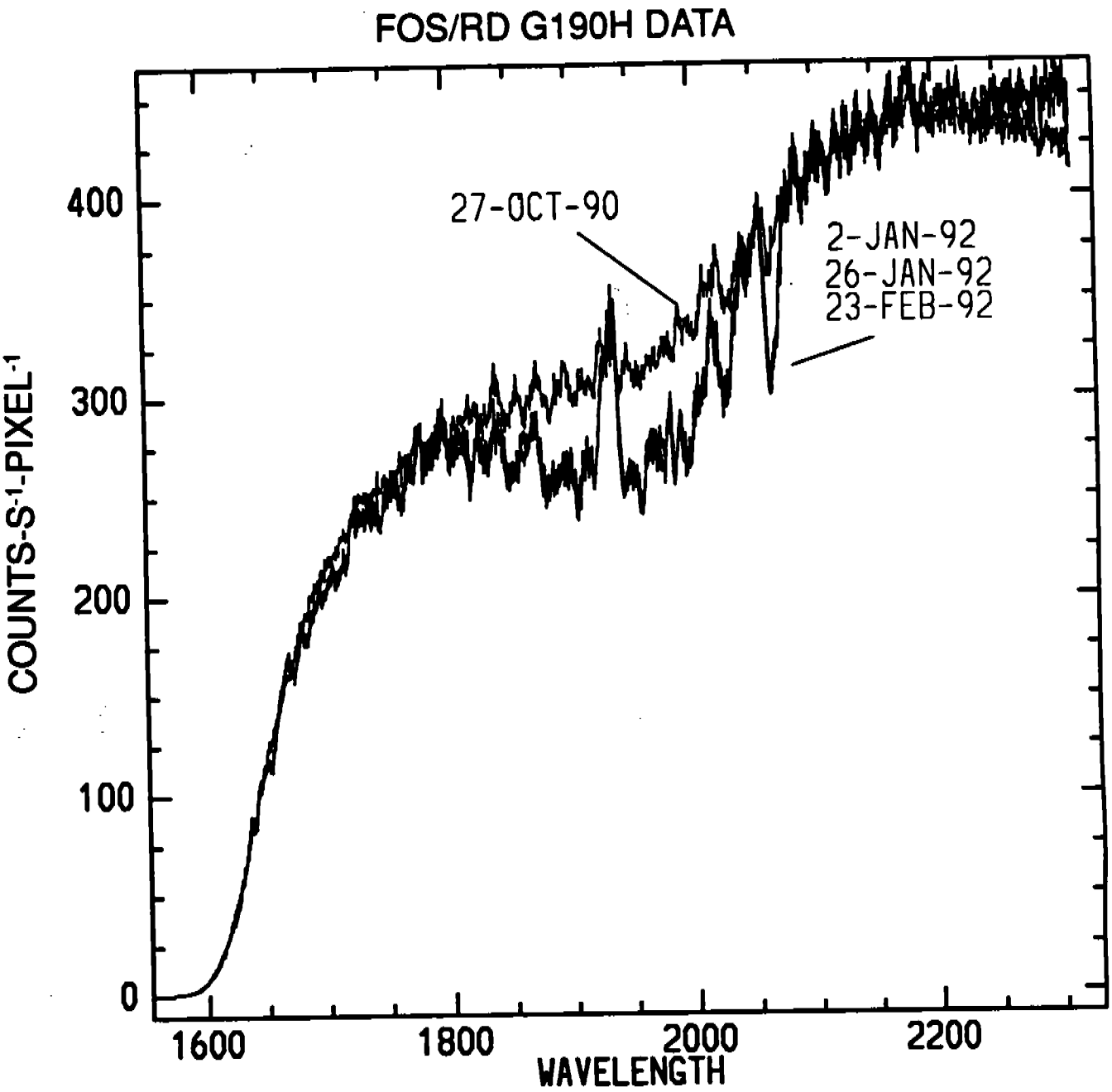

Figure 3.3.2: Redside G190H Data of target G191-B2B from which the Flat Fields are produced.

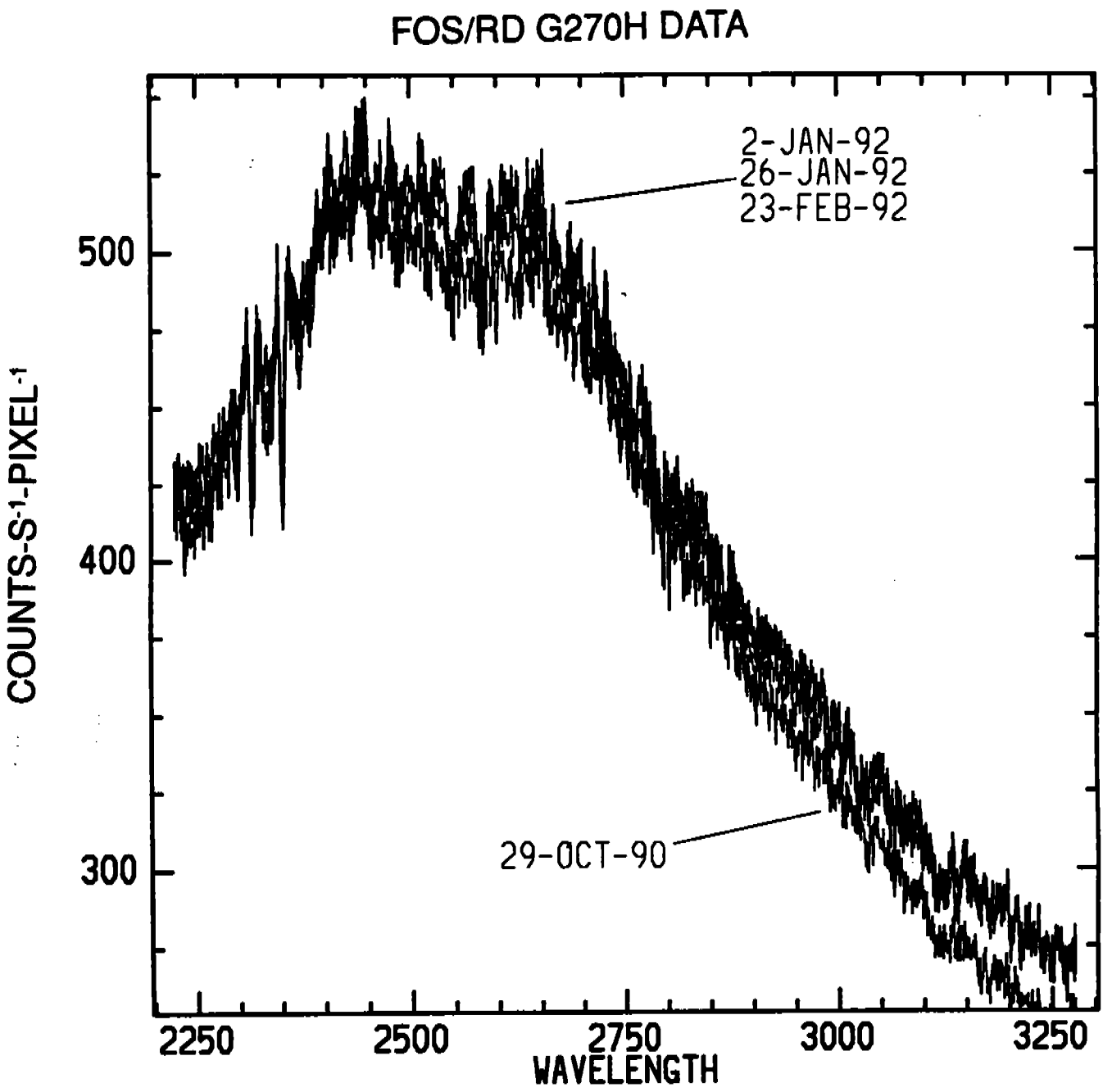

Figure 3.3.3: Redside G270H Data of target G191-B2B from which the Flat Fields are produced.

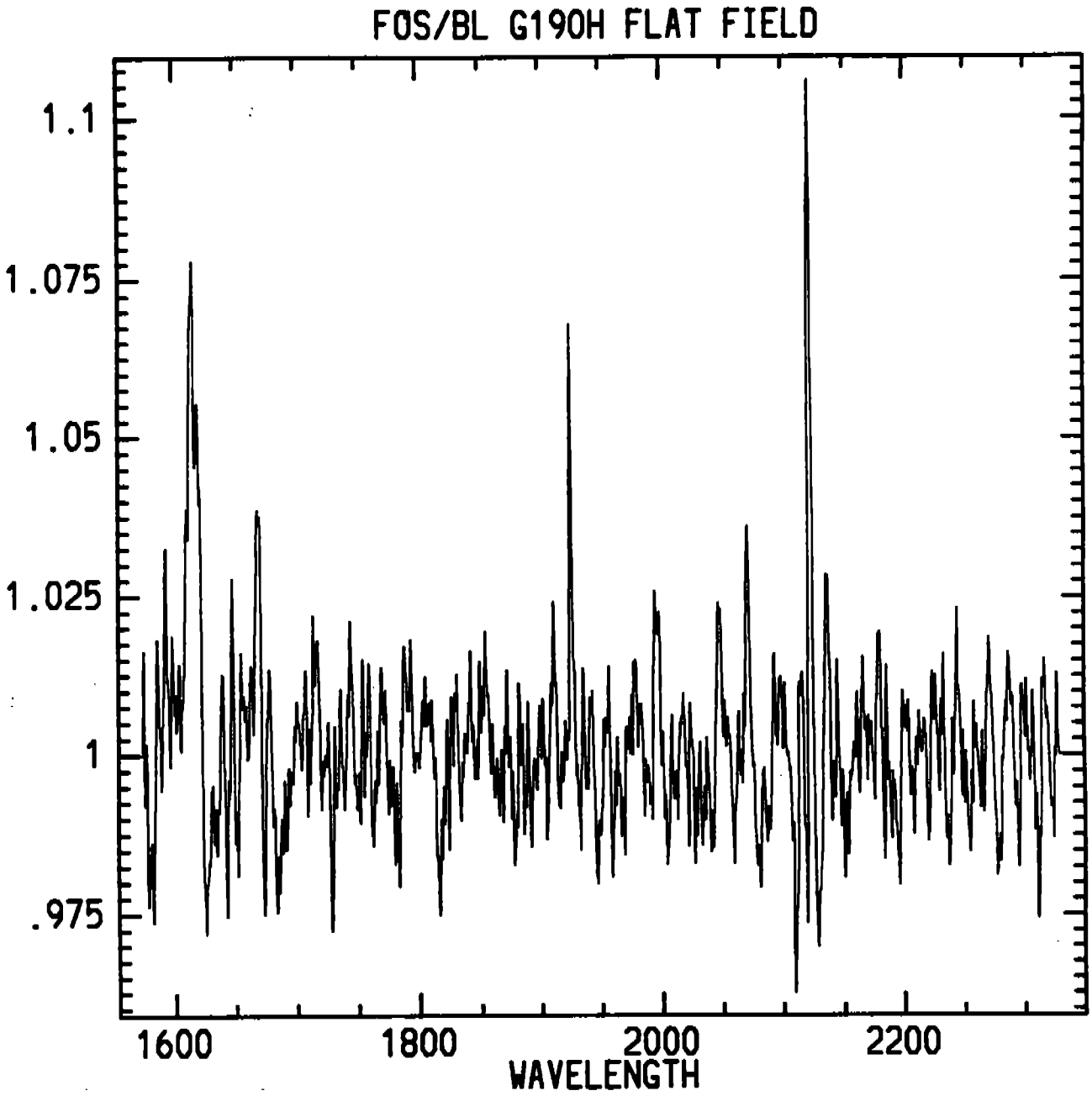

Figure 3.3.4: Blueside G190H Flat Field of target G191-B2B from September 1991.

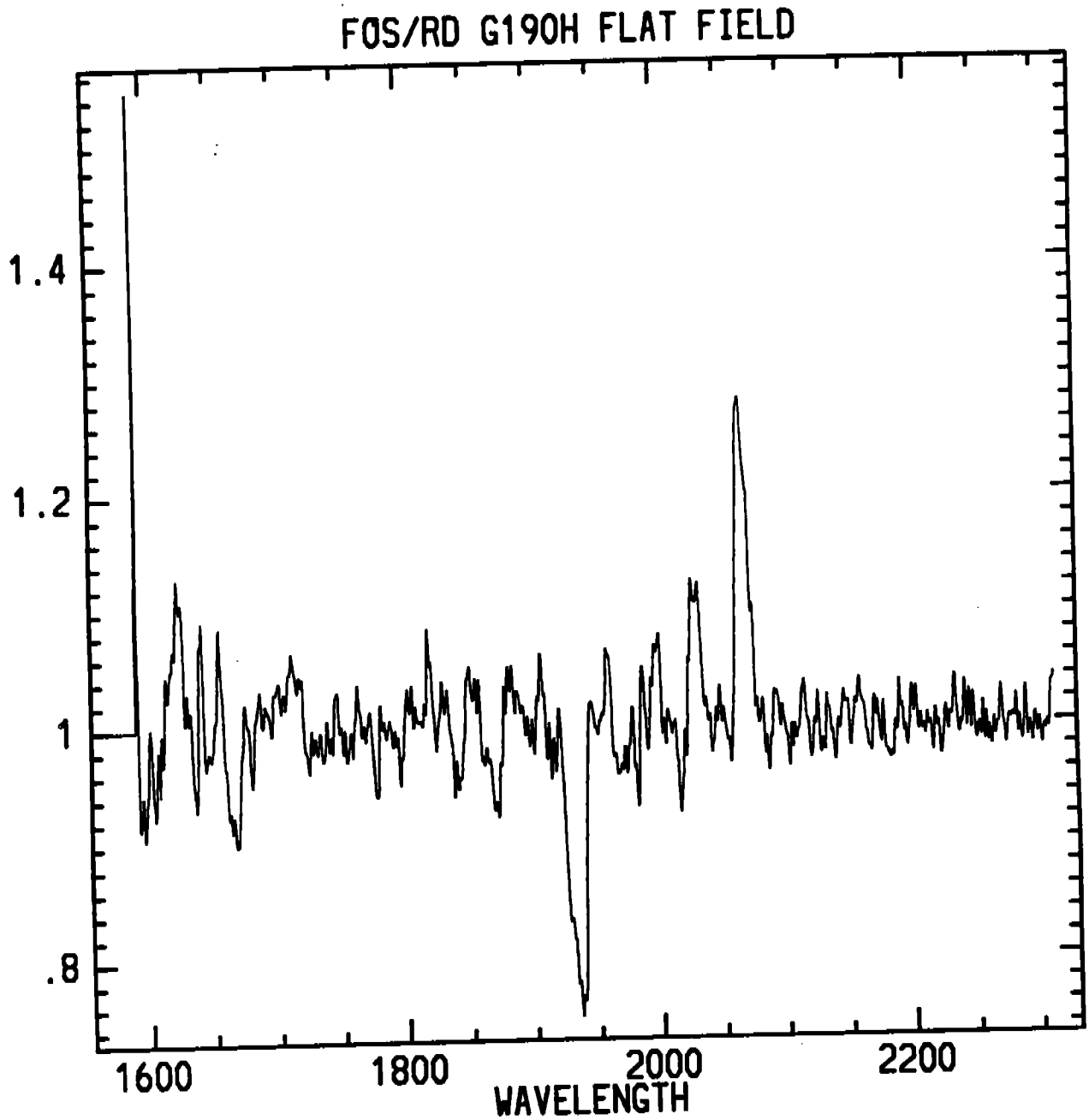

Figure 3.3.5: Redside G190H Flat Field of target G191-B2B from January 26, 1992.

4.0 SIMULATING FOS

A simulator developed by K. Horne is available in the ST ScI Data Analysis System (STSDAS) in the package **synphot** (see ST ScI Newsletters Vol. 7, No. 2 and 3 for brief descriptions by K. Horne, and Synphot Users Guide, by D. Bazell, Nov. 1990, ST ScI.) XCAL, a version of the simulator which is compatible with VAX/VMS machines, can be copied from the ST ScI Electronic Information Service (STEIS) via an anonymous ftp account (for instructions on logging into STEIS, see Reppert, December 1990, ST ScI Newsletter Vol. 7 No. 3, page 16).

Synphot can be used to "observe" an interactively determined input spectrum with any FOS configuration to produce a spectrum of detector counts s^{-1} $diode^{-1}$. This can be done in the package **plspec**, by setting the observing mode, the input spectrum, the form of the output, and the wavelength dispersion of the output spectrum.

For example, to reproduce the detected counts s^{-1} $diode^{-1}$ plot for the blue side of grating G190H shown in Figure 1.2.3, the parameters in **plspec** would be set as given in Table 4.1, with the observing mode set with the parameter "obsmode = fos, blue, g190h, 4.3", the input spectrum set with the parameter "spectrum = flam 1.e-14," the units for the plot to be produced set by the parameter "form = counts", and the wavelength resolution of the resulting plot set with the parameter "wavetab = g190hb.dat".

The observing mode is simply the instrument (fos), followed by the side (red or blue), followed by the grating (of the gratings available in Table 1.1.1), followed by the aperture. The **form** of the plot can be **fnu** (F_ν = erg s^{-1} cm^{-2} Hz^{-1}), **flam** (F_λ = erg s^{-1} cm^{-2} $Å^{-1}$), **photnu** (detected counts s^{-1} cm^{-2} Hz^{-1}), **photlam** (detected counts s^{-1} cm^{-2} $Å^{-1}$), **counts** (detected counts s^{-1} cm^{-2} $pixel^{-1}$), or **abmag** (Magnitude = $-2.5\log$(fnu) - 48.60).

For calculating signal–to–noise ratio, **counts** is the best option for the parameter **form**, with a pixel defined as a resolution element. When using **counts**, the pixel size is determined by the **wavetab** parameter. A series of tables are available which correspond to the wavelength dispersion of the diodes of the FOS gratings, where a diode is a resolution element. These tables are invoked with "wavetab=g190hb.tab", for example for the G190H grating on the blue side.

Synphot and XCAL also contain the stars in the Bruzual, Person, Gunn, & Stryker Atlas (not yet published) which covers a full range of spectral types. To see the stars available in **synphot**, change your default directory to the Atlas (cd crgirdbpgs) and type dir. Then, an Atlas star can be selected for the input spectrum for example by setting "spectrum = crgridbpgs$bpgs_1.tab", for the first star.

A power law spectrum can also be input into **plspec**. For example, as a test, a power law of form $F_\nu \propto \nu^{-\alpha}$, with $\alpha = 2$, normalized to the value $F_\lambda = 1.0 \times 10^{-14}$ erg s^{-1} cm^{-2} $Å^{-1}$ can be used. This gives the same result as the case given in Table 4.1, with a constant value for F_λ, and thus demonstrates how to input a power law normalized to a flux in the ultraviolet. The command is "spectrum = pl 1900 2 rn "box 1900 1" flam 1.e-14." In this example, the power law is designated by **pl**, at 1900Å, with a slope of **-2**. This power law is renormalized **rn** to the bandpass 1Å wide at 1900Å which is defined in double quotes by **"box 1900 1"**. The renormalization value is given by "flam 1.e-14". The renormalization could have been given in any of the units available for the units of the plot.

Both synphot and XCAL use the updates to instrument sensitivities as they are produced.

Table 4.1
Example parameters in SYNPHOT to reproduce Figure 1.2.3

Parameter	Setting	Definition
obsmode	**fos,blue,g190h,4.3**	Observation mode or @filelist
spectrum	**flam 1.e-14**	Synthetic spectrum or @filelist
spfile	none	Spectrophotometry data
pfile	none	Photometry data
form	**counts**	Form for output graph
ebmv1	0.	First E(B-V) value
ebmv2	0.	Last E(B-V) value
nebmv	1.	Number of E(B-V) values
device	stdgraph	Output device
left	**1400.**	x value for left side of graph
right	**2400.**	x value for right side
bottom	**0.**	y value for bottom
top	**4.**	y value for top
errtype	n	n[one] p[oints] c[ontinuous] v[ertical] h[oriz]
wavetab	**g190hb.dat**	Wavelength table name
refdata		Reference data
mode	h	

5.0 ACKNOWLEDGEMENTS

I would particularly like to thank George Hartig for reading and discussing the contents of this handbook in detail. I would like to thank Cindy Taylor and Bidushi Bhattacharya for producing most of the tables and the plots. I would like to thank Ralph Bohlin and Don Neill for providing plots of detected count rates. I would like to thank Guest Observers K. Horne and A. Koratkar for providing examples of exposure logsheets. I would like to thank Bill Baity for ensuring that I received all copies of Science Verification reports from FOS team members as soon as they were available. A number of people improved the handbook by reading and commenting on the text. For this generous contribution I would like to thank Bram Boroson, Ross Cohen, Ian Evans, Mingsheng Han, Buell Jannuzi, Vesa Junkkarinen, Tony Keyes, Ray Lucas, and Ruth Peterson.

6.0 REFERENCES

Allen, R.G., & Angel, J.R.P. 1982, *FOS Spectropolarimeter Performance, FOS Instrument Handbook*, Version 1, ST ScI, page C-1.

Allen, R.G., & Smith, P.S. 1992, *FOS Polarimetry Calibrations*, Instrument Science Report CAL/FOS-078.

Anderson, S.F. 1992, *FOS Spectral Flat Field Calibration*, Instrument Science Report CAL/FOS-075.

Caldwell, J., & Cunningham, C.C. 1992, *Grating Scatter in the FOS and the GHRS*, Science Verification 1343 Interim Report.

Ford, H.C. 1985, *FOS Instrument Handbook*, ST ScI.

Harms, R.J. 1982, *The Space Telescope Observatory*, ed. D.N.B. Hall, (Special Session of Commission 44, IAU General Assembly, Patras, Greece, August, 1982; NASA CP-2244).

Harms, R.J., Angel, R., Bartko, F., Beaver, E., Bloomquist, W., Bohlin,R., Burbidge, E.M., Davidsen, A.,F., Flemming, J.C., Ford, H., & Margon, B. 1979, *SPIE*, **183**, 74.

Hartig, G.F. 1989, *Faint Object Spectrograph Instrument Handbook Supplement No. 1*, ST ScI.

Kriss, G.A., Blair, W.P., & Davidsen, A.F. 1991, *In-Flight FOS Wavelength Calibration – Template Spectra*, Instrument Science Report CAL/FOS-067.

Kriss, G.A., Blair, W.P., & Davidsen, A.F. 1992, *Internal/External Offsets in the FOS Wavelength Calibration*, Instrument Science Report CAL/FOS-070.

Lindler, D., & Bohlin, R. 1986, *FOS Linearity Corrections*, Instrument Science Report CAL/FOS-025.

Morris, S.L., Weymann, R.J., Savage, B.D., & Gilliland, R.L. 1991 *Ap. J. (Letters)*, **377**, L21.

Mount, G., & Rottman, G. 1981, *The Solar spectral irradiance 1200–3184Å near solar maximum: July 15, 1980*, J. Geophys. Res. **86**, 9193.

Rosenblatt, E.I., Baity, W.A., Beaver, E.A., Cohen, R.D., Junkkarinen, V.T., Linsky, J.B., and Lyons, R.W. 1992, *An Analysis of FOS Background Dark Noise*, Instrument Science Report CAL/FOS-071.

Wegener, R., Caldwell, J., Owne, T., Kim, S.J., Encrenaz, T., & Comber, M. 1985 *The Jovian Stratosphere in the Ultraviolet, Icarus*, **63**, 222.

APPENDIX A. TAKING DATA WITH FOS

To ensure that the reader is always confused, two sets of nomenclature will be used here to describe the taking of FOS data – those used in the exposure logsheets to command observations, and those used in the FOS data headers. (It goes without saying that the exposure logsheets and the data headers do not use the same words to describe the same things.) Table A.1 gives the translation between the two, together with defaults and definitions.

FOS observations are performed in a nested manner, with the smallest unit being the livetime of the instrument plus the deadtime (LT + DT). Table A.1 lists the parameters in the order in which FOS observations are nested. Standard spectra are taken by sub–stepping the diode array along the dispersion in the X direction, and then by performing the sub–stepping five times over adjacent diodes to minimize the impact of dead diodes. The sequence is then

$$(\mathrm{LD} + \mathrm{DT}) \times 4 \times 5.$$

The minimum livetime is 0.003 seconds. The minimum livetime plus deadtime is 0.030 seconds. Using the minimum livetime results in very inefficient observations, where data is being taken only $0.003/0.03 = 0.1$ of the time.

The user has access only to those parameters that can be set in the exposure logsheet. For example, the user cannot set the livetime, but the user can set the product of livetime and INTS (STEP-TIME = LT× INTS). Likewise, the user cannot explicitly set the deadtime, but in PERIOD mode, the user can set the ratio of livetime to deadtime (DATA-RATIO = LT/DT).

For the most common mode, ACCUM, an FOS integration is constructed in the order

$$\Delta t = (\mathrm{LT} + \mathrm{DT}) \times \mathrm{INTS} \times \mathrm{NXSTEPS} \times \mathrm{OVERSCAN} \times \mathrm{YSTEPS} \times \mathrm{NPATT} \times \mathrm{NREAD}$$

where NXSTEPS = SUB-STEP, and YSTEPS = Y-SIZE. This equation also gives the elapsed time for the observation, which for standard ACCUM mode is equal to

$$\Delta t = (\mathrm{LT} + \mathrm{DT}) \times \mathrm{INTS} \times 4 \times 5 \times 1 \times \mathrm{NPATT} \times \mathrm{NREAD}.$$

NPATT, the number of patterns, is set after the setting of sub–step, overscan, and ystep, to achieve the exposure time requested. When NPATT has reached the maximum that it can be set to, a value of 256, then INTS is incremented. Obviously, this must be done in an optimal way to ensure that the efficiency ($\propto$ LT/DT) remains high. The maximum value for INTS is also 256.

For a RAPID observation, an FOS integration is built up in a slightly different order:

$$\Delta t = (\mathrm{LT} + \mathrm{DT}) \times \mathrm{INTS} \times \mathrm{NXSTEP} \times \mathrm{OVERSCAN} \times \mathrm{YSTEPS} \times \mathrm{NPATT} \times \mathrm{NMCLEARS}$$

which is usually equal to

$$\Delta t = (\mathrm{LT} + \mathrm{DT}) \times \mathrm{INTS} \times 4 \times 5 \times 1 \times \mathrm{NPATT} \times \mathrm{NMCLEARS}.$$

However, the sub–stepping, the overscan values, and the wavelength range can be lowered in RAPID to accommodate shorter time between the taking of spectra.

For a PERIOD observation, an FOS integration is built up of

$$\Delta t = (\mathrm{LT} + \mathrm{DT}) \times \mathrm{INTS} \times \mathrm{NXSTEP} \times \mathrm{OVERSCAN} \times \mathrm{YSTEPS} \times \mathrm{SLICES} \times \mathrm{NPATT}$$

Table A.1
FOS Observing Parameters
Listed in Order of Execution

Exposure Logsheet	FOS Header	Default	Definition
—	LIVETIME	0.512 sec	(LT) Time FOS is integrating.
—	DEADTIME	0.010 sec	(DT) Overhead time.
—	INTS	—	Number of times to execute (LT+DT)
SUB-STEP	NXSTEP	4	Number of steps of size diode/NXSTEP in direction of dispersion.
COMB	OVERSCAN*	YES	Whether or not to execute x stepping to remove the effects of dead diodes. For COMB= YES, MUL=5. For COMB= NO, MUL=1.
Y-SIZE	YSTEPS	1	Number of steps perpendicular to dispersion.
BINS	SLICE	5	For PERIOD only, equal to 1 otherwise. Number of bins to divide one period into.
—	NPATT	—	Number of times to execute the pattern so as to achieve the exposure time.
—	NREAD	—	For ACCUM only, equal to 1 otherwise. For readouts short enough to correct for GIMP
—	NMCLEARS	—	For RAPID only, equal to 1 otherwise. Number of times to clear data so as to read new data.

* The FOS header value for OVERSCAN is equal to the value for MUL.

Additional FOS Observing Parameters

Exp.Log.	FOS	Default	Definition
STEP-TIME	LT×INTS	0.5	Available in RAPID and PERIOD.
DATA-RATIO	LT/DT	Maximum	Available in PERIOD only.

where SLICES = BINS. As with RAPID, x step and overscan values can be lowered to result in a greater number of SLICES (BINS).

These equations give the elapsed time of an observation and so they can be used to calculate the actual start time of any observation, by subtracting them from the first packet time (FPKTTIME) which is given in the group parameter at the beginning of every group of "multi-group" data.

$$\text{Start Time} = \text{FPKTTIME} - \Delta t$$

The start time of the entire observation is also given in the data header as EXPSTART. Note that all times in the header, including the first packet time, and the start time, are given in units of Modified Julian Date, which is the Julian date minus 2400000.5. The Modified Julian Date for 1992 is given by:

$$\text{MJD} = 48621.0 + \text{day of year} + \text{fraction of day from } 0^h UT.$$

APPENDIX B. DEAD DIODE TABLES

Occasionally one of the 512 diodes on the red or the blue side becomes very noisy, or ceases to collect data. Since launch, the FOS has lost 3 diodes on the blue side and 2 diodes on the red side. In addition, several diodes on each side became noisy and have been disabled. When a diode goes bad in orbit, there is a delay time before that diode behavior is discovered, and another delay time before that diode is disabled so that its effect is removed from the data. Table B.1 lists the current (as of April 13, 1992) list of disabled diodes. Table B.2 lists the history of the diodes that have been disabled, when they were discovered to be bad, and when they were removed from action. Note that the channels are numbered in this table from 0 to 511, while they are numbered in the STSDAS tasks from 1 to 512.

Table B.1
FOS DEAD AND NOISY CHANNEL SUMMARY[1]

BLUE DETECTOR

DISABLED Dead Channels	DISABLED Noisy Channels	DISABLED Cross-Wired Channels	ENABLED But Possibly Noisy
49	31	47	
101	73	55	
223	201		
284	218		
409	225		
441	235		
471	241		
	268		
	398		
	451		
	465		
	472		
	497		
	427[a]		

a. Active 4/13/92

RED DETECTOR

DISABLED Dead Channels	DISABLED Noisy Channels	ENABLED But Possibly Noisy
2	110	261
6	189	380
29	285	412
197	405	153
212	409	
486		

1. Diode range is 0-511.

Table B.2
FOS DEAD AND NOISY CHANNELS HISTORY[1]

BLUE DETECTOR

DISABLED Dead Channels	DATE Died	DATE Disabled
49	2/17/88	2/17/88
101	8/28/91	12/14/91
223	4/6/88	4/6/88
284	2/17/88	2/17/88
409	2/17/88	2/17/88
441	6/20/91	8/3/91
471	6/1/91	8/3/91

DISABLED Noisy Channels	DATE Noticed	DATE Disabled
31	3/11/88	11/1/90
73	Prelaunch	Prelaunch
201	Prelaunch	Prelaunch
218	Prelaunch	Prelaunch
225	?	5/18/90,(enabled 6/11/90),11/1/90
235	10/1/90	11/1/90
241	10/3/90	11/1/90
268	Prelaunch	Prelaunch
398	12/90	2/20/91
451	Prelaunch	Prelaunch
465	Prelaunch	Prelaunch
472	Prelaunch	Prelaunch
497	3/11/88	11/1/90
219	Prelaunch	Prelaunch,ENABLED 2/20/91
415	Prelaunch	Prelaunch,ENABLED 2/20/91
427	3/5/92	Pre-launch,(enabled 2/20/91),4/13/92

RED DETECTOR

DISABLED Dead Channels	DATE Died	DATE Disabled
2	Prelaunch	Prelaunch
6	Prelaunch	Prelaunch
29	10/27/91	1/7/92
197	12/90	2/20/91
212	Prelaunch	Prelaunch
486	Prelaunch	Prelaunch

DISABLED Noisy Channels	DATE Noticed	DATE Disabled
110	7/16/90	9/14/90
189	9/91	12/14/91
285	Prelaunch	Prelaunch (formerly DEAD)
405	Prelaunch	Prelaunch
409	Prelaunch	Prelaunch
235	Prelaunch	Prelaunch,ENABLED 8/27/90
261	Prelaunch	Prelaunch,ENABLED 8/27/90
344	Prelaunch	Prelaunch,ENABLED 8/27/90
381	Prelaunch	Prelaunch,ENABLED 8/27/90

1. Diode range is 0-511.

APPENDIX C. A COMPARISON OF GHRS AND FOS SENSITIVITIES

R. Gilliland & G. F. Hartig

from ST ScI Newsletter, Nov. 1991, Vol. 8, no. 3, p. 13

To facilitate changes that may be necessary for Cycle 1 proposals that currently use the GHRS side 1 low-resolution grating, G140L, but will be changed to the FOS, the following table provides a direct comparison of GHRS and FOS photometric sensitivities for point sources well centered in the aperture.

The sensitivities in columns 2, 3, and 4 are expressed in counts^{-1} diode^{-1} per (erg s^{-1} cm^{-2} Å^{-1}).

For the GHRS with the G140L grating, column 2 gives the sensitivity with the 2″.0 square Large Science Aperture (LSA). For observations with the Small Science Aperture (SSA), the GHRS sensitivity should be multiplied by the ratio in the final column. With G140L the diode spacing is 0.572 Å, and the resolutions of the SSA and LSA are 1.1 and 2.0 diodes, respectively.

The FOS sensitivities are also on a per–diode basis, for the 1″.0 – diameter circular aperture. The diode spacings are 1″.0Å and 1.46Å for the G130H and G190H gratings, respectively, and the resolution of the 1″.0 aperture is 1.4 diodes.

A sample calculation: at 1200Å, one would infer from the above that GHRS G140L was a factor of 5 faster than FOS *on a per–diode basis.* On a per–Ångstrom basis, the ratio at 1200Å is 8.9. But the FOS does have greater wavelength coverage, and starts gaining ground rapidly with increasing wavelength in terms of relative sensitivity.

Throughputs for the various FOS apertures at 1500 Å, as determined from direct comparison on a point source, are as follows:

Aperture (arcsec)	Throughput
1.4×4.3	49%
1.0	27%
0.5	20%
0.3	13%
0.25×	20%

The GHRS to FOS ratios derived from the table should typically be within 20% of truth, allowing for good exposure–time planning.

Table C.1
GHRS and FOS Sensitivities

Wavelength	GHRS G140L[a]	FOS/BL G130H	FOS/BL G190H	GHRS SSA/LSA[b]
1100	1.81×10^{11}[c]	0.00	-	0.19
1150	2.90×10^{12}	2.79×10^{11}	-	0.20
1200	7.75×10^{12}	1.53×10^{12}	-	0.21
1250	1.28×10^{13}	3.47×10^{12}	-	0.22
1300	1.45×10^{13}	4.57×10^{12}	-	0.22
1350	1.53×10^{13}	5.70×10^{12}	-	0.23
1400	1.45×10^{13}	6.50×10^{12}	-	0.23
1450	1.18×10^{13}	7.90×10^{12}	-	0.24
1500	9.24×10^{12}	9.41×10^{12}	-	0.24
1550	7.35×10^{12}	1.16×10^{13}	-	0.25
1600	5.27×10^{12}	1.37×10^{13}	1.83×10^{13}	0.25
1650	4.61×10^{12}	-	2.19×10^{13}	0.26
1700	3.79×10^{12}	-	2.50×10^{13}	0.26
1750	2.41×10^{12}	-	2.89×10^{13}	0.27
1800	1.25×10^{12}	-	3.45×10^{13}	0.27
1850	4.39×10^{12}	-	3.90×10^{13}	0.28
1900	1.29×10^{11}	-	4.50×10^{13}	0.28

a. This is for the LSA (2.0 arcsec square)
b. This is the expected SSA/LSA sensitivity.
c. All sensitivites are in: $\frac{\text{cts/s/diode}}{\text{ergs/s/cm}^2\text{/A}}$

APPENDIX D. GRATING SCATTER

This appendix reports the results of tests analyzed by Caldwell & Cunningham (1992) on the red scattered light which contaminates blue side observations of FOS.

The FOS blue side detector is sensitive to visible wavelengths (see Figure 1.0.1) and is therefore susceptible to grating scatter. Grating scatter significantly affects FOS spectra of red objects below 2100Å. Grating scatter tests (Caldwell & Cunningham 1992) compare GHRS spectra in the G140L (central wavelength 1700Å), G270M (2300–3220Å), and G200M (1800–2185Å) gratings with FOS blue side observations of G190H (1570–2330), G270H (2230–3300Å), and G160L (1150–2520Å). Because GHRS is solar blind, the spectra produced by GHRS can show the degree to which red scattered light impacts blue spectra taken with the FOS. Although the test was done with the blue side, the red side of FOS, which has a higher blue sensitivity than the blue side and no attenuation of red sensitivity, has an appreciably greater scatter problem.

The G2V star 16 Cyg B was observed. Because 16 Cyg B is a solar analog, the solar spectrum can be used for an approximate independent check on the HST observations of 16 Cyg B. 16 Cyg B is determined to be a solar analog at wavelengths longer than 3000Å, so it may be intrinsically different than the sun in the ultraviolet. The spectra of 16 Cyg B from GHRS, and FOS, and the Solar spectrum from a rocket by Mount and Rottman (1981) is shown in the Figure D.1, reproduced from Caldwell, and Cunningham (1992). As can be seen in Figure D.1, the flux in the FOS spectrum increases strongly toward wavelengths below 2100Å relative to the true flux. This is because the blue spectrum decreases rapidly with shorter wavelengths, so the relative contribution from scattered light increases towards shorter wavelength.

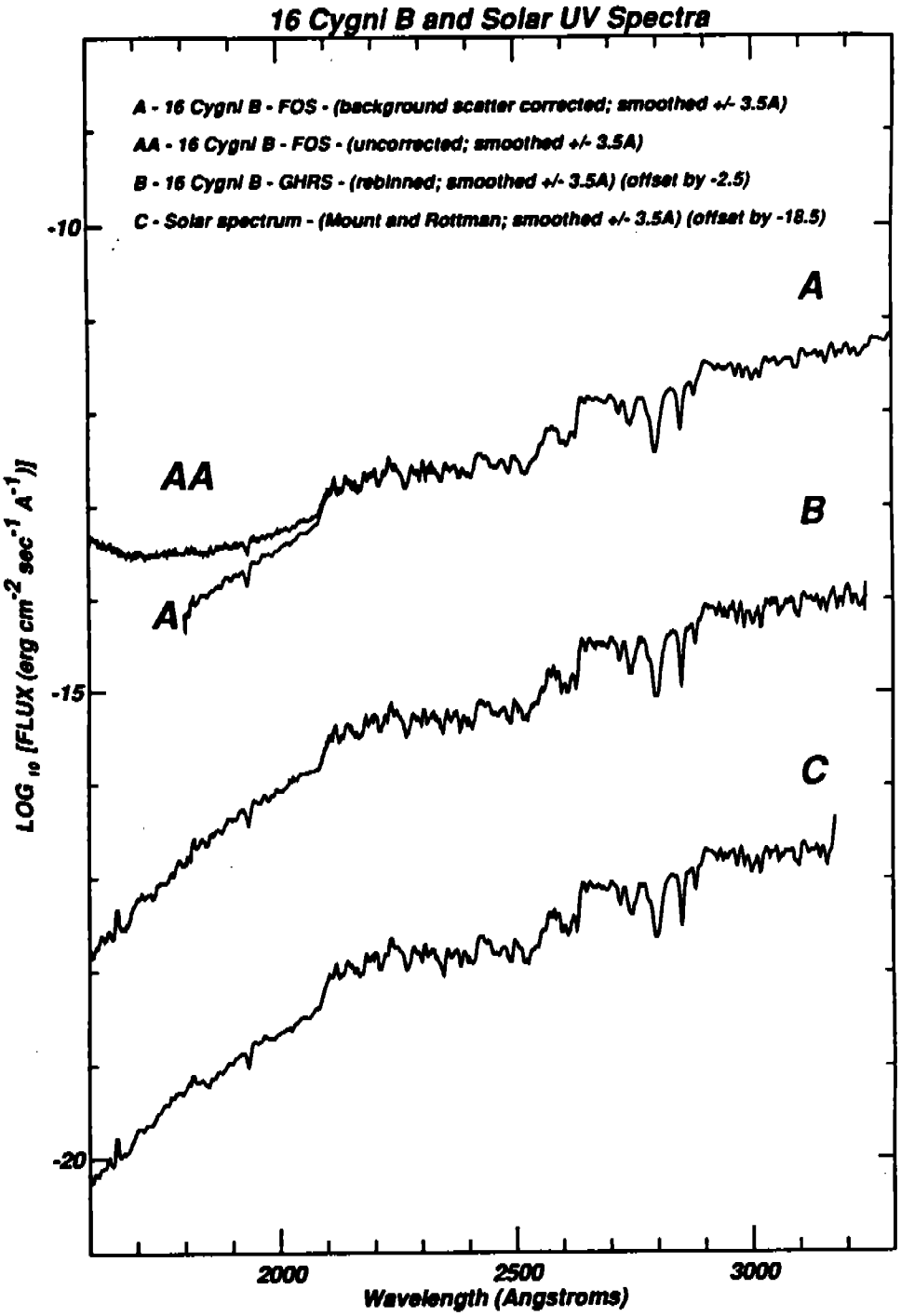

Figure D.1: Comparison of FOS and GHRS 16 Cyg B HST spectra with a solar rocket UV spectrum by Mount and Rottman (1981), as modified by Wagener *et al.* (1985). The FOS uncorrected spectrum (curve AA) is a composite of the G190H and G270H FOS observations. Curve A is a replot of these data after a correction for grating scatter has been applied. A composite spectrum of all the GHRS spectra is plotted as curve B. The modified Mount and Rottman (1981) solar data is plotted as curve C.

APPENDIX E. EXPOSURE LOGSHEETS

1 TAR NUM	2 TARGET NAME	3 TARGET DESCRIPTION	4 TARGET POSITION	5 COORD EQNX	6 PM PR	7 RADIAL VEL.	8 ACQUI PRBLM	9 SPEC PLATE RQ AV	FLX REF	10 FLUX DATA
1	3C298 QUASAR	E,314	RA-OFF= 8.785' +/- 0.3", DEC-OFF= 20.9' +/- 0.3", FROM 2						1	V= 16.79, E(B-V)= 0.2
2	3C298-OFFSET COMMENTS: A5 STAR USED FOR OFFSET.	A,126	RA= 14H 16M 30S +/- 1", DEC= +6D 42' 0" +/- 1"	1950					1	V=15
3	M81	E,301,919	RA= 9H 51M 30S +/- 10", DEC= +69D 18.3' +/- 10"	1950					1	V=18,E(B-V)=0.2
4	M81-OFFSET COMMENTS: TO BE FOUND - OFFSET STAR.	A	RA-OFF= 0.05S +/- 1', DEC-OFF= 0' +/- 1, FROM 3, TBD-EARLY							
5	BRIGHT_STAR	A,111	RA= 2H 16M 28S +/- 1", DEC= +43D 51' 56" +/- 2"	1950					1	V=11,TYPE=B3V,E(B-V)=0.5
6	QUASAR	E,314	RA= 12H 34M 56.7S +/- 1", DEC= +12D 34.5' +/- 1"	1950					1	V=16
7	AE-AQR	A,151,154,161	RA= 20H 40M 9.02S +/- 0.5", DEC= -0D 52' 15.5" +/- 0.5", PLATE-ID=02C4	J2000	N				1	V= 10.8 +/- 1.1
8	0405-123	E,314	RA= 4H 5M 27.45S +/- 1", DEC= -12D 19' 31.8" +/- 1"	1950					1	V=14.82
9	3C273	E,314	RA= 12H 26M 33.25S +/- 1", DEC= +2D 19' 43.2" +/- 1"	1950					1	V=12.86

1 LN NM	2 SEQ NAME	3 TARGET NAME	4 INSTR CONFIG	5 OPER. MODE	6 APER OR FOV	7 SPECTRAL ELEMENT	8 CENTRAL WAVELN	9 OPTIONAL PARAMETERS	10 NUM EXP	11 TIME	12 S/N	13 FLX REF	14 PR	15 SPECIAL REQUIREMENTS
1.000		3C298-OFFSET	FOS/RD	ACQ/BINARY	4.3	MIRROR		BRIGHT=330000, FAINT=3300	1	3.3S		1	3	ONBOARD ACQ FOR 2 ; CYCLE 2 / 1-19;
2.000		3C298	FOS/RD	ACCUM	0.5	G780H	7800		1	60S	10	1	3	
3.000		3C273	FOS/RD	ACQ/BINARY	4.3	MIRROR		BRIGHT=330000, FAINT=6600	1	4.7S		1	3	ONBOARD ACQ FOR 4 ; SEQ 3-4.3 NO GAP;
4.000		3C273	FOS/RD	ACQ/PEAK	0.25X2.0	MIRROR			1	4.7S			1	ONBOARD ACQ FOR 4 .1-4.3; SPATIAL SCAN;
4.100		3C273	FOS/RD	ACCUM	0.25X2.0	G190H			1	300S			1	
4.200		3C273	FOS/BL	ACQ/PEAK	0.25X2.0	MIRROR			1	1.0S			1	ONBOARD ACQ FOR 4 .3; SPATIAL SCAN;
4.300		3C273	FOS/BL	ACCUM	0.25X2.0	G130H			1	300S			1	
5.000		M81	WFC	IMAGE	ALL	F606W			1	60S		1	1	EARLY ACQ FOR 6-8 ;
6.000		M81-OFFSET	FOS/BL	ACQ/BINARY	4.3	MIRROR			1	TBD		1	1	SEQ 6-8 NO GAP; ONBOARD ACQ FOR 7-8;
7.000		M81	FOS/BL	ACCUM	0.3	G190H	1900		1	3000S	50	1	1	
8.000		M81	FOS/BL	ACQ	4.3	MIRROR			1	63S		1	1	
9.000		SATELLITE	FOS/RD	ACQ/PEAK	4.3	G570H	5700		1	1S		1	2	ONBOARD ACQ FOR 10; SPATIAL SCAN;
10.000		SATELLITE	FOS/RD	ACQ/PEAK	1.0	G570H	5700		1	1S		1	2	ONBOARD ACQ FOR 10.1; SPATIAL SCAN ;
10.100		SATELLITE	FOS/RD	ACQ/PEAK	0.5	G570H	5700	SCAN-STEP=0.35, SEARCH-SIZE=3	1	1S			2	ONBOARD ACQ FOR 10.2; SPATIAL SCAN ;
10.200		SATELLITE	FOS/RD	ACCUM	1.0	G570H	5700		1	1M			2	

1 LN NM	2 SEQ NAME	3 TARGET NAME	4 INSTR CONFIG	5 OPER. MODE	6 APER OR FOV	7 SPECTRAL ELEMENT	8 CENTRAL WAVELN	9 OPTIONAL PARAMETERS	10 NUM EXP	11 TIME	12 S/N	13 FLX REF	14 PR	15 SPECIAL REQUIREMENTS
10.300		BRIGHT_STAR	FOS/RD	ACQ/PEAK	4.3	G570H	5700		1	1S			1	ONBOARD ACQ FOR 10.4; SPATIAL SCAN ;
10.400		BRIGHT_STAR	FOS/RD	ACQ/PEAK	1.0	G570H	5700		1	1S			1	ONBOARD ACQ FOR 10.5; SPATIAL SCAN ;
10.500		BRIGHT_STAR	FOS/RD	ACQ/PEAK	0.5	G570H	5700	SCAN-STEP=0.35, SEARCH-SIZE=3	1	1S			1	ONBOARD ACQ FOR 10.6;
10.600		BRIGHT_STAR	FOS/RD	ACCUM	1.0	G570H	5700		1	1M			1	
11.000		AE-AQR	FOS/BL	ACQ/BINARY	4.3	MIRROR		BRIGHT=200000 FAINT=1680	1	0.66S		1	1	ONBOARD ACQ FOR 12-13 ; GROUP 11-13 NO GAP ;
	COMMENTS: BRIGHT VARIABLE STAR. UV MAY VARY BY 1MAG IN 10MIN. 0.26S GIVES 300 X 11 COUNTS. FAINT = 660 X 0.66 / 0.26, BRIGHT = MAXIMUM ALLOWED.													
12.000		AE-AQR	FOS/BL	RAPID	4.3	G160L		READ-TIME=4	1	300M			1	
	COMMENTS: 9.88 HR BINARY PERIOD TAKES 7 OR MORE CONSECUTIVE HST ORBITS. 5H EXPOSURE ASSUMES 45M PER HST ORBIT. 4S READOUTS FOR FLARES, AND 16.5S OSCILLATIONS. PLEASE INCREASE EXPOSURE TO FILL OUT COMPLETE HST ORBIT WINDOWS.													
13.000		AE-AQR	FOS/BL	RAPID	4.3	PRISM		READ-TIME=4	1	37M			1	
	COMMENTS: RAPID READOUT REQUIRED FOR FLARES, AND 16.5 AND 33 SEC OSCILLATIONS. OK TO LENGTHEN EXPOSURE TO FILL OUT COMPLETE HST ORBIT WINDOWS.													
14.000		0405-123	FOS/BL	ACQ/BINARY	4.3	MIRROR			1	3.8S	17	13	1	ONBOARD ACQ FOR 15; COND IF GIMP FIX NOT DONE ; SEQ 14-19 NO GAP;
	COMMENTS: MANUAL MERGE 14.0 AND 15 INTO SAME ALIGNMENT													
15.000		0405-123	FOS/BL	ACCUM	4.3	G130H	1300	POLSCAN=4B	1	1300S	90	13	1	COND IF GIMP FIX NOT DONE ;
16.000		0405-123	FOS/BL	ACCUM	4.3	G130H	1300	POLSCAN=4B	1	2300S	90	13	1	COND IF GIMP FIX NOT DONE ;
17.000		0405-123	FOS/BL	ACCUM	4.3	G130H	1300	POLSCAN=4B	1	2300S	90	13	1	COND IF GIMP FIX NOT DONE ;

1 LN NM	2 SEQ NAME	3 TARGET NAME	4 INSTR CONFIG	5 OPER. MODE	6 APER OR FOV	7 SPECTRAL ELEMENT	8 CENTRAL WAVELN	9 OPTIONAL PARAMETERS	10 NUM EXP	11 TIME	12 S/N	13 FLX REF	14 PR	15 SPECIAL REQUIREMENTS
18.0 00		0405-123	FOS/B L	ACCUM	4.3	G130H	1300	POLSCAN=4B	1	2300S	90	1 3	1	COND IF GIMP FIX NOT DONE ;
19.0 00		0405-123	FOS/B L	ACCUM	4.3	G130H	1300	POLSCAN=4B	1	2300S	90	1 3	1	COND IF GIMP FIX NOT DONE ;

Scan Parameters Form

Data ID : 1
Exposure logsheet lines: 4,4.2
FGS Scan: Continuous (C) or Dwell (D): D Dwell only: Dwell points/line: 7 Seconds/dwell: 1.000
Scan width (arc-sec): 0.0000 Scan length (arc-sec): 0.4000 Angle between sides (degrees): 0.0000
Number of lines: 1 Scan rate (arc-sec/sec): 0.0000 PA of first scan line (degrees): 90.0000
Scan Frame (CEL or S/C): S/C Length Offset (arc-sec): 0.2000 Width Offset (arc-sec): 0.0000

Data ID : 2
Exposure logsheet lines: 9
FGS Scan: Continuous (C) or Dwell (D): D Dwell only: Dwell points/line: 2 Seconds/dwell: 1.000
Scan width (arc-sec): 7.0000 Scan length (arc-sec): 4.3000 Angle between sides (degrees): 90.0000
Number of lines: 6 Scan rate (arc-sec/sec): 0.0000 PA of first scan line (degrees): 90.0000
Scan Frame (CEL or S/C): S/C Length Offset (arc-sec): 2.1500 Width Offset (arc-sec): 3.5000

Data ID : 3
Exposure logsheet lines: 10
FGS Scan: Continuous (C) or Dwell (D): D Dwell only: Dwell points/line: 6 Seconds/dwell: 1.000
Scan width (arc-sec): 0.7000 Scan length (arc-sec): 3.5000 Angle between sides (degrees): 90.0000
Number of lines: 2 Scan rate (arc-sec/sec): 0.0000 PA of first scan line (degrees): 90.0000
Scan Frame (CEL or S/C): S/C Length Offset (arc-sec): 1.7500 Width Offset (arc-sec): 0.3500

Data ID : 4
Exposure logsheet lines: 10.3
FGS Scan: Continuous (C) or Dwell (D): D Dwell only: Dwell points/line: 3 Seconds/dwell: 1.000
Scan width (arc-sec): 0.0000 Scan length (arc-sec): 2.8000 Angle between sides (degrees): 90.0000
Number of lines: 1 Scan rate (arc-sec/sec): 0.0000 PA of first scan line (degrees): 0.0000
Scan Frame (CEL or S/C): S/C Length Offset (arc-sec): 1.4000 Width Offset (arc-sec): 0.0000

Data ID : 5
Exposure logsheet lines: 10.4
FGS Scan: Continuous (C) or Dwell (D): D Dwell only: Dwell points/line: 6 Seconds/dwell: 1.000
Scan width (arc-sec): 0.7000 Scan length (arc-sec): 3.5000 Angle between sides (degrees): 90.0000
Number of lines: 2 Scan rate (arc-sec/sec): 0.0000 PA of first scan line (degrees): 90.0000
Scan Frame (CEL or S/C): S/C Length Offset (arc-sec): 1.7500 Width Offset (arc-sec): 0.3500
